Published in final edited form as:
Dev Biol. 2008 February 15; 314(2): 300–316.

Distribution of RNA Binding Protein MOEP19 in the Oocyte Cortex and Early Embryo Indicates Pre-patterning Related to Blastomere Polarity and Trophectoderm Specification

John C. Herr*, **Olga Chertihin**, **Laura Digilio**, **Kula Nand Jha**, **Soumya Vemuganti**, and **Charles J. Flickinger**

Center for Research in Contraceptive and Reproductive Health, Department of Cell Biology, University of Virginia, Charlottesville, VA, 22908

Abstract

We report the cloning and characterization of MOEP19, a novel 19 kDA RNA binding protein that marks a defined cortical cytoplasmic domain in oocytes and provides evidence of mammalian oocyte polarity and a form of pre-patterning that persists in zygotes and early embryos through the morula stage. MOEP 19 contains a eukaryotic type KH-domain, typical of the KH-domain type I superfamily of RNA binding proteins, and both recombinant and native MOEP19 bind polynucleotides. By immunofluorescence, MOEP19 protein was first detected in primary follicles throughout the ooplasm. As oocytes expanded in size during oogenesis MOEP 19 increased in concentration. MOEP 19 localized in the ovulated egg and early zygote as a symmetrical spherical cortical domain underlying the oolemma, deep to the zone of cortical granules. MOEP 19 remained restricted to a cortical cytoplasmic crescent in blastomeres of 2, 4 and 8 cell embryos. The MOEP19 domain was absent in regions underlying cell contacts. In morulae, the MOEP19 domain was found at the apex of outer, polarized blastomeres but was undetectable in blastomeres of the inner cell mass. In early blastocysts, MOEP19 localized in both mural and polar trophectoderm and a subset of embryos showed inner cell mass localization. MOEP19 concentration dramatically declined in late blastocysts. When blastomeres of 4-8 cell stages were dissociated, the polarized MOEP19 domain assumed a symmetrically spherical localization, while overnight culture of dissociated blastomeres resulted in formation of re-aggregated embryos in which polarity of the MOEP19 domain was re-established at the blastomere apices. MOEP19 showed no evidence of translation in ovulated eggs, indicating *MOEP19* is a maternal effect gene. The persistence during early development of the MOEP 19 cortical oocyte domain as a cortical crescent in blastomers suggests an intrinsic pre-patterning in the egg that is related to the apical-basolateral polarity of the embryo. Although the RNAs bound to MOEP19 are presently unknown, we predict that the MOEP19 domain directs RNAs essential for normal embryonic development to specific locations in the oocyte and early embryo.

Keywords

MOEP19; oocyte pre-patterning; RNA binding protein; blastomere apical-basal polarity; maternal effect gene; early embryo; trophectoderm; inner cell mass

*Corresponding Author: John C. Herr, Department of Cell Biology, P.O. Box 800732, University of Virginia Health System, Charlottesville, Virginia 22908, Phone: (434) 924-2007, Fax (434) 982-3912, E-mail: jch7k@virginia.edu

Introduction

A current controversy in mammalian developmental biology is whether there exists in oocytes any spatially restricted developmental information that influences or directs early embryogenesis (Johnson, 2001). In frogs, mollusks, nematodes and tunicates the presence of morphogenetic determinants within the egg cytoplasm and the redistribution of these determinants during egg development, fertilization and early cleavage are well known to play a role in determining fates of individual cells (Nishida, 1992). In oocytes of the tunicates *Styela partita* (Conklin, 1905) and *Halocynthia roretzi* (Nishida, 1987), for example, the ooplasm is segregated into fortuitously pigmented regions that after fertilization apportion into various blastomeres. The yellow cytoplasmic crescent has been observed to give rise to muscle cells; the grey equatorial crescent produces the notochord and neural tube; the animal cytoplasm becomes the larval epidermis; while the yolky grey vegetal region has been shown to give rise to the larval gut (Nishida, 1994). In Drosophila, gradients of maternal transcription factors are spatially restricted in the egg and provide cis-regulation of zygotic genes (Nusslein-Volhard, 1991). Asymmetries in mRNA in the animal and vegetal poles of Xenopus eggs reflect subsequent patterning during morphogenesis, particularly segregation of the germ plasm (King et al, 2005).

The concept is thus well established in several invertebrate and vertebrate species that asymmetries in information laid down in the egg and reorganized at fertilization drive cell fates and play a role in such processes as the development of the major body axes (Rossant, 2004). To date, however, there has been limited evidence in mammalian oocytes for an informative molecular mosaicism in the ooplasm, zygote or blastomeres of two and four cell embryos that might predict later developmental events in a manner comparable to the regional differentiation of egg cytoplasm in other species.

One view of early mammalian development is that the mammalian oocyte possesses spherical symmetry and lacks the polarity evident in frogs and insects, and, moreover, that the blastomeres of at least the first three cleavages remain equipotent in the mouse. Time-lapse recordings of early mouse development, for example, have suggested that there is no specification in the oocyte of the animal-vegetal axis of the embryo (Hiiragi and Solter, 2004). Of note however, these authors report that in their mouse embryos, the polar body was not attached. Thus, in the absence of a way to mark the animal pole of the embryos studied the authors may not have a definitive axis of reference. Further evidence against oocyte polarity includes an analysis of the cleavage planes in two cell embryos revealing that they are ordered randomly (Louvet-Vallee et al, 2005). However, other groups report that the divisions are commonly perpendicular to each other: one along the AV axis and another perpendicular to it (Gardner, 2002; Piotrowska-Nitsche and Zernicka-Goetz, 2005).

This view of an early mouse embryo lacking definitive polarity is supported by its ability to tolerate many kinds of experimental manipulation, such as the removal at the 2 cell stage of one blastomere, with subsequent development of a complete, normal fetus. Similarly, the insertion of blastomeres or ES cells results in viable chimeras (Tarkowski, 1959,1961,1967, 2001;Rossant, 1976). Even removal of the animal or the vegetal pole of the oocyte does not prevent development (Zernicka-Goetz, 1998), which has argued against the existence of localized determinants in the ooplasm (Zernicka-Goetz, 2005). Recent in vitro time-lapse imaging and in vivo lineage labeling of two cell embryos has provided evidence that the E-Ab axis of the mouse blastocyst is generated independently of early cell lineage. The embryonic-abembryonic axis is attributed to the elliptical shape of the zona pellucida and rotational movements of the embryo within the zona (Kurotaki, et al, 2007). It is noteworthy that the ability of the mouse embryo to regulate for loss or reorganization of cells does not preclude the presence of molecular mosaicism.

Other authors have provided evidence in support of pre-patterning, particularly forms of prepatterning related to embryonic-abembryonic axis formation and asymmetries in the information content of blastomeres. Gardner, using a non-invasive technique for focal marking the zona pellucida, has argued that the embryonic-abembryonic axis of the blastocyst is already specified in the zygote by the onset of cleavage (Gardner, 2001). Other authors have suggested that at the two cell stage it is already possible to predict which cell will contribute a greater proportion of progeny to the abembryonic or embryonic parts of the blastocyst (Piotrowska et al, 2001). The two-cell stage blastomere that is the first to divide has been proposed to preferentially contribute progeny to the embryonic part of the blastocyst when its division is meridional, but not equatorial (Piotrowska et al., 2001, Piotrowska-Nitsche and Zernicka-Goetz, 2005). Chimaeras constructed of four-cell stage blastomeres that resulted from late second cleavages failed to develop to term suggesting certain four-cell blastomeres differ in their developmental properties (Piotrowska-Nitsche et al., 2005). Histone3 methylation at specific arginine residues is higher in those four cell blastomeres predicted to contribute to the inner cell mass and polar trophectoderm (Torres-Padilla et al., 2007). This finding might suggest that blastomeres that inherit the vegetal part of the egg might have different epigenetic modifications and significantly different developmental potential from cells which will inherit the animal part of the egg.

Blastomere polarization is considered by several authors to appear first in the 8 cell mouse embryo during compaction, the process whereby the inner cell mass lineage diverges from the trophectoderm lineage (Johnson and McConnell, 2004). During compaction, blastomeres flatten upon one another through establishment of E-cadherin-mediated cell contacts (Fleming et al, 2001); cytoplasmic components such as clathrin-coated vesicles, endosomes and microfilaments become asymmetrically distributed (Johnson and Maro, 1986); microvilli disappear from cell contacts and become restricted to the surface of the apical pole (Louvet et al, 1996; Louvet-Vallee et al 2001); nuclei move to the basal region; and the cytoskeleton is reordered. In accord with this view, the murine proteins PARD3, PARD6b, EMK1, and PKCζ, which are associated with the establishment of polarity in various cells and with asymmetric divisions in oocytes of *Caenorhabditis* and *Drosophilia*, show no asymmetric distribution prior to compaction in the mouse (Thomas et al, 2004, Plusa et al, 2005, Vinot et al, 2005). Thus, several authors conclude that the first developmentally relevant asymmetries are set up during compaction (Vinot et al, 2005) and it is in the compacting late eight cell embryo that differentiation of the first polarized proto-epithelium begins.

In the transition from 8 to 16 cells in the mouse embryo, orientation of the spindle with respect to the apical-basal axis is thought to be random. Thus, some asymmetrical divisions occur in which one daughter cell inherits a large part of the apical pole and becomes trophoblast, whereas the other daughter cell, which lacks microvilli and is adherent to it neighbors, becomes an inner cell (Johnson and Maro, 1986; Johnson and McConnell, 2004). In this way, two different cell types with distinct fates are generated after the fourth cleavage: external polarized cells that will give rise to the trophectoderm and internal non-polarized cells that will produce the inner cell mass in the blastocysts (Fleming, 1987; Johnson and Ziomek, 1981).

Despite evidence that both supports and contraves the idea of oocyte prepatterning, experimental data to date remains compatible with some form of spatially restricted developmental information being pre-positioned in the mammalian oocyte in the form of proteins or other cellular constituents. Recently we initiated a proteomic approach that identified novel oocyte proteins that may shed light on the question of mammalian oocyte pre-patterning. Previous findings that mRNA gradients in lower species associate with cortical crescents (Swalla and Jefferey, 1995) and with movements of germ plasm (King et al 2005) suggest that if mRNA is indeed segregated in the murine oocyte, then mammalian RNA binding proteins in the ooplasm may display developmentally meaningful morphogenetic patterns.

Because many previous studies have failed to uncover molecular asymmetries (Johnson and McConnell, 2004), we adopted microsequencing and bioinformatic strategies that focused on un-annotated oocyte genes possessing RNA binding motifs. Here we provide evidence for an early form of molecular asymmetry within the murine oocyte cytoplasm by following the maternal gene product, MOEP 19, a member of the superfamily of KH domain RNA binding proteins. MOEP19 is a natural biomarker for a region of oocyte cortex, the MOEP19 domain, that reveals an intriguing form of pre-patterning in the oocyte cytoplasm and an intrinsic oocyte polarity that relates to the subsequent apical-basolateral polarity of blastomeres from the first cleavage through the morula. Previous data in the field is discussed in light of the present evidence for mammalian oocyte pre-patterning and its role in early embryogenesis.

Materials and Methods

Isolation of Triton X-114 soluble egg proteins and 2D gel analysis

Eight hundred zona free mouse oocytes were treated with solubilization buffer containing Triton X-114 according to the manufacturer's instructions [Pierce, Rockford, IL]. The detergent soluble fraction was incubated at 37° C for 10 minutes resulting in phase partitioning (Bordier, 1981) of detergent (upper layer) and aqueous (low layer) phases. The sample was centrifuged at 13,000 x g. The detergent phase was further enriched for proteins using the Pierce kit resin and analyzed by 2D gel electrophoresis after suspension in membrane lysis buffer. Triton X-114 soluble proteins were separated by isoelectric focusing on IPG strips (pH range 3-10 nonlinear) followed by electrophoresis on a gradient gel (8-16 % acrylamide). Proteins were silver stained and cored for further analysis by tandem mass-spectrometry.

Tandem Mass Spectrometry of Egg Peptides

Silver stained protein spots were cored from 2D SDS-PAGE gels, fragmented, destained in methanol, reduced in 10 mM dithiothreitol, and alkylated in 50 mM iodoacetamide in 0.1 M ammonium bicarbonate. The gel pieces were then incubated with 12.5 ng/ml trypsin in 50 mM ammonium bicarbonate overnight at 37°C. Peptides were acetonitrile and 5% formic acid and microsequenced by tandem mass spectrometry at the Biomolecular Research Facility of the University of Virginia. In the case of the acidic ~18.6 kDa (~ pI 5.2) MOEP19 isoform, spots corresponding to those recognized by immunoblotting with anti-rec MOEP19 serum were identified by staining with protogold after immunoreaction, compared to silver stained gels, and then cored from silver stained gels for microsequencing.

Immunoblotting

Protein samples for 1-D gel SDS PAGE were prepared by homogenizing tissues in Laemmli buffer (Laemmli, 1970) containing a cocktail of protease inhibitors (Sigma) under non-reducing conditions. Four percent β-Mercaptoethanol was added to supernatant fractions before gel loading. Protein extracts of mouse oocytes were prepared by boiling zona free oocytes in Laemmli buffer. Proteins were separated on 12 % SDS-polyacrylamide gels and immunoblotted onto PVDF membranes. After blocking in 5 % non-fat milk (in Tris-Buffered Saline with 0.1 % Tween) membranes were incubated with rat anti- recombinant MOEP19 immune and pre-immune serum (1:1000 dilution in 5 % non-fat milk). Subsequently, blots were incubated with HRP-conjugated goat anti-rat IgG (1:5000). Specific antibody interactions were visualized with enhanced chemiluminescence or TMB.

Recombinant protein expression and purification

A PCR product encoding the open reading frame of MOEP19 (492 amino acids plus a 6-his tag at the C terminus) was amplified from mouse oocyte cDNA and cloned into Nco1 and EcoR1 sites of the pET28b expression vector (Novagen, San Diego, CA). The construct was

confirmed by sequencing and transformed into E. coli BL21 DE3 cells (Stratagene, La Jolla, CA). 20 L cultures were grown in the presence of ampicillin until optical density reached 0.6. Expression was induced with 1 mM IPTG and cells were cultured for 4 hours. The expression of MOEP19 was assessed by analysis of bacterial proteins on an SDS-polyacrylamide gel followed by Coomassie blue staining and Ni-NTA blotting. Bacterial cells were harvested and soluble and insoluble fractions were analyzed for the presence of MOEP19. The majority of the expressed MOEP19 was present in inclusion bodies. A bacterial cell lysate was prepared by using urea buffer, and recombinant MOEP19 was purified in a two step process of affinity chromatography followed by isoelectric focusing in a Prep Cell [BioRad]. Peak fractions containing recombinant MOEP19 were concentrated using Centricon's YM 10 and dialyzed against PBS. The purity of the recombinant protein was determined by 1-D SDS PAGE and staining with Coomassie Blue and silver.

Production of rat anti-MOEP19 sera and IgG purification

Preimmune sera were collected from 5 rats prior to injections. Four animals were injected with recombinant MOEP19 three times at 2 week intervals, while one control animal received adjuvant alone. For the first injection an emulsion of 100 μg of purified recombinant MOEP19 was prepared with Freund's complete adjuvant. Freund's incomplete adjuvant was used for two subsequent booster immunizations. At each immunization three equal portions of the immunogen were injected into three sites: subcutaneously into the suprascapular fat pad and intramuscularly into the quadracepts of each hind leg. Animals were sacrificed 10 days after the last injection, and serum was separated. The serum was tested for specificity by immunoblotting on the recombinant protein and protein extracts from mouse oocytes. A specific band at ~19 kDa was observed in mouse oocyte extract, consistent with the molecular weight of the recombinant protein. Anti-MOEP19 IgG was purified using the Melon gel specifically designed by Pierce for purification of rat IgG. Purified IgG was precipitated by $(NH_4)_2SO_4$, resuspended in purification buffer (provided with Melon gel) and dialyzed against 30 mM PBS. The concentration of rat IgG was estimated spectrophotometrically at 280 nm.

RNA isolation and RT-PCR

Mouse tissues, including heart, lung, liver, kidney, spleen, thymus, testis, pancreas and ovary were submersed in Trizol solution (1 ml of Tri-reagent per 100 mg of tissue) immediately after collection. Tissues were homogenized using a separate RNA free tip (IKA Works, Inc.) for each tissue. 0.2 ml of chloroform was added per 1 ml of Trizol, and the sample was separated into three layers by centrifugation. The upper aqueous layer was collected, RNA was precipitated by adding 0.5 ml of isopropyl alcohol per 1 ml of Tri-Reagent and the samples were incubated at -20°C overnight. Samples were centrifuged at 12,000 rpm for 15 minutes, supernatants were removed, and RNA pellets were washed once in 75 % ethanol, dried and resuspended in 30-100 ul of DEPC water. Isolated total RNA was quantified by UV absorption at 260 nm. 1 μg of purified RNA from each tissue was used for cDNA synthesis by reverse transcription. The cDNA equivalent of 70 ng RNA was used for PCR amplification of MOEP19. Amplification of beta actin was used as a control for RNA loads in each tissue.

PCR amplification of MOEP19

Mouse oocyte cDNA was reversed transcribed using RNA isolated from 300 oocytes. Primers were designed based on RIKEN cDNA sequence matching peptides obtained from microsequencing analysis of the spot from 2D gel. PCR was performed directly from 5 μl of first-strand cDNA using 1.25 ng of MOEP19-forward (5′-AGCTTTGAAAAGCGAGACCA-3′) and MOEP19-reverse (5′-TCAAACCAACAGCATACCAAA-3′) primers and the Advantage 2 PCR Enzyme System (BD Biosciences). The amplified product of correct size was cloned into pCR 2.1 TOPO vector

(Invitrogen) and the consensus sequence was defined by sequencing purified DNA product from 12 colonies to assure the absence of random mutations.

Staging and collecting eggs and embryos

Germinal vesicle oocytes as well as oocytes from immature follicles were collected from ovaries of 25-30 gram female ICR mice. Follicles were punctured with a 26 gauge needle to release oocytes into a 900 μl drop of Whitten's media containing 0.2 mM IBMX to prevent germinal vesicle breakdown. Oocytes were then washed and fixed in 4% paraformaldehyde for 20 min and quenched with NH_4Cl for 15 min. Mature, metaphase II eggs were collected from superovulated females (10 IU of PMSG followed by 10 IU hCG 48 h later). Twelve hours after hCG injection, oocytes were released from the oviducts into Whitten's media containing 0.05% hyaluronidase to remove cumulus cells. Eggs were then washed, fixed and quenched as above. For pronuclear stage embryos, oviducts were harvested from mated superovulated females approximately 18 h after hCG injection. Embryos were released from the oviducts into M2 media containing 0.05% hyaluronidase and either fixed and quenched as above or cultured at 37°C in M16 medium in 5% CO_2 to obtain later developmental stages. In addition to studies of embryos developed in vitro, embryos at various stages were obtained 20-60 hours post coitus by flushing the oviducts of mated females with 0.1 ml of M2 medium in a 1 ml syringe attached to a 26-gauge needle.

Indirect Immunofluorescence

Ovaries were collected from 2 and 6 week old mice and fixed in 4% paraformaldehyde. Five micron paraffin sections were made and processed for immunofluorescence. Slides were rehydrated and blocked for 30 min in PBS containing 10% NGS. Slides were incubated with a 1:100 dilution of preimmune or immune sera diluted in PBS + 1% NGS overnight at 4°C. Slides were washed with PBS and incubated with a 1:200 dilution of goat anti-rat rhodamine labeled IgG (Jackson Immuno-Research Labs Inc.) for 1 h at room temperature. Slides were washed, mounted and imaged on a Zeiss Axiovert 200 inverted fluorescent microscope equipped with a Diagnostic Instruments 4.1 digital camera and SPOT Insight software.

Oocytes and embryos were fixed in 4% paraformaldehyde, permeabilized with 0.5% TritonX-100 in PBS for 10 min at room temperature and then blocked with PBS containing 0.1% Tween 20 and 3% BSA for 30 min. The specimens were incubated for 1 h with a 1:100 dilution of preimmune or anti-MOEP19 serum diluted in PBS containing 0.1% Tween 20 and 1.5% BSA. Oocytes and embryos were washed and then incubated with Cy3 conjugated goat anti-rat IgG, $F(ab')_2$ fragment specific secondary antibody (Jasckson Immuno-Research Labs, West Grove, PA) diluted in PBS/Tween for 30 min at room temperature.

The samples were then washed and placed in 0.4 mg/ml RNAse in PBS with 1% BSA for 30 min, stained with 20 ηM Sytox (Molecular Probes, Eugene, OR) for 10 min, incubated in slow fade (Molecular Probes, Eugene, OR) equilibration media for approximately 1 min and then mounted on slides in slow fade mounting media. Images were obtained on a Zeiss 410 Axiovert 100 microsystems LSM confocal microscope. Standardization of images was accomplished by holding constant attenuation, contrast, brightness and the pin hole aperture. Four second scans were averaged four times per line using a 40X oil lens and a standard zoom factor of 2.5.

In vitro Phosphorylation of Recombinant MOEP19

Recombinant MOEP19 was incubated with purified PKA catalytic subunit (100 units) or purified casein kinase II (0.12 units) at 30°C for 15 min in a phosphorylation reaction mix containing 20 mM Hepes (pH 7.4), 10 mM $MgCl_2$, 10 mM $MnCl_2$, protease inhibitor mix (without EDTA), 100 μM Na_3VO_4, 5 mM p-nitrophenyl phosphate, 40 mM β-glycerophosphate, 2 μCi γ^{32}P-ATP, 1% Triton X-100 and 1 mg/ml BSA. Recombinant

MOEP19 alone and enzyme (PKA and CKII) alone controls were included in the experiments. The phosphorylation reaction was stopped by adding Laemmli buffer immediately after the incubation period. The phosphorylation of specific proteins by radiolabeled ATP was then analyzed by subjecting the entire reaction mixture to SDS-PAGE analysis followed by autoradiography.

^{35}S methionine labeling of oocytes and 2-cell embryos

One hundred oocytes and 100 2-cell embryos were cultured in 100 μl of media with 100 μCi of [35S]-labeled methionine at 37° C for 2 hours. Oocytes and embryos were washed 3 times with PBS to remove unincorporated radioactive methionine. Eggs and embryos were lysed using lysis buffer (20 mM Tris, 1 mM EDTA and 0.5 % Triton X-100) and centrifuged at 13,000 x g. Supernatants were precleared with normal rabbit serum and Protein A sepharose. Precleared supernatants were incubated with anti-MOEP19 rat serum (1:100) for 2 hours at 4° C, and protein G agarose was used to pull down rat IgG. Beads were washed 5 times with PBS and immunoprecipitates were eluted by boiling beads in the sample buffer. The immunoprecipitates were separated by 1-D SDS PAGE and analyzed by autoradiography. Western blotting was employed to confirm MOEP19 precipitation in the sample.

Homoribopolymer Binding Assay

Binding of recombinant MOEP19 and endogenous MOEP19 in oocyte lysate to homopolymers was performed under conditions previously described (Filipenko et al., 2004). Lysates extracted from 50 mouse oocytes using 0.5 % Triton X-100 and 50 ng of purified recombinant MOEP19 were added directly to the poly(U) agarose beads (Sigma) and incubated at 4° C for 1 hour. In parallel, 50 ng of recombinant protein were preincubated with 5 μg of poly(U), added to poly(U) agarose beads, and incubated at 4° C for 1 hour on a shaker. The beads were washed 3 times with TBS/Triton X-100, boiled in Laemli buffer with, or without mercaptoethanol, and analyzed by Western blot using anti-MOEP19 rat serum, followed chemiluminescence and autoradiography.

Results

Identification of MOEP-19 in 2-D Egg Proteome

The hydrophobic protein extract of 800 zona-free oocytes was separated on a 2D gel, silver stained, and a prominent spot of mw ~ 19 kDa, pI 6 was cored from the gel, digested with trypsin and analyzed by tandem mass spectrometry yielding five peptides (Fig.1). Searched against the NCBI database, these peptides were predicted to arise from an unnamed protein [later designated MOEP19 for mouse oocyte and early embryo protein] deduced from the mouse RIKEN cDNA sequence NM_026480 (Katayama et al, 2005). An EST database search revealed 26 transcripts for MOEP19 in fertilized eggs and the early mouse embryos with two ESTs noted in thymus and one in the pituitary gland.

MOEP19 Cloning and Orthologues

PCR amplification from mouse oocyte RNA (strain ICR) yielded a 492 bp open reading frame encoding a 164 aa protein (Fig. 2). Compared with RIKEN cDNA NM_026480 (Katayama et al, 2005), MOEP19 had two nucleotide substitutions, only one of which led to a replacement: of glutamine-163 with leucine. GenBank accession number DQ238107 was assigned to this MOEP19 clone. The calculated mass of 18.5 kDa and pI 5.8 (ExPaSy pi/MW tool) closely matched the mass of 19 kDa and pI of 6 estimated for the spot cored and microsequenced from the 2D protein gel.

Each of the five peptides obtained by ms/ms microsequencing the 2-D gel protein spot was identified embedded within the deduced amino acid sequence of DQ238107 [Fig. 1], confirming that the authentic cDNA corresponding to the cored spot had been cloned. Using the BLAST algorithm, the MOEP19 amino acid sequence revealed 25 % identity and 54 % similarity (Fig. 2) to NM_ 025274, developmental pluripotency protein 5 [Dppa5] also known as embryonal stem cell specific gene 1 (Esg-1: Bierbaum et al 1994). The KH RNA-binding motif (Siomi et al, 1994) present in Dppa5 was identified in MOEP19 (see below). The MOEP19 chromosomal locus at 9E1 has been sequenced as Genbank clone RP24-160H16 (unpublished; deposited by Birren, B., Nusbaum, C. and Lander, E.). Dppa 5 is located in the same region as the MOEP19 locus on mouse chromosome 9 while the human orthologue of MOEP19 and human Dppa5 genes are located in a syntenic region at 6q13.

MOEP19 orthologs in rat, cow, dog and man were identified by bioinformatic analyses (Fig. 2). Mouse and rat MOEP19 are 68% identical and 82 % similar; mouse and cow MOEP are 45 % identical and 71 % similar; while the comparisons with dog [60% and 82%] and man [55% and 79%] indicate that relatively little divergence has occurred in the MOEP19 sequence over evolutionary time. The region showing the highest conservation among the 5 species was found between amino acids 20 and 120. Query of the SUPERFAMILY database (Madera et al, 2004) placed MOEP19 in the eukaryotic type KH-domain (KH-domain type I) superfamily of RNA binding proteins. The region of highest conservation among the species contained the predicted KH superfamily motif extending from aa 40-150 (Madera et al, 2004).

Analysis of hydrophobic and hydrophilic amino acids in mouse MOEP19 with SOUCI yielded an average hydrophobicity of -0.204878, predicting that MOEP19, lacking other post-translational modifications, is a soluble cytosolic protein. MOEP19 contained 3 predicted sites for potential phosphorylation by protein kinase C [residues 16-18, 26-28, 142-144], two predicted sites for casein kinase II phosphorylation [66-69, 160-163] and three potential N-myristolation sites [59-64, 93-98, 145-150].

Immunoreagent Development and MOEP19 Microheterogeneity

Polyclonal anti-serum produced in rats to recombinant mouse MOEP19 immunoreacted with both recombinant MOEP19 and MOEP19 extracted from mouse eggs, while the preimmune serum and the adjuvant alone control serum recognized neither the recombinant protein nor any protein band in egg protein extracts (Suppl Fig, 1). These results indicated that epitopes in the “native” MOEP19 were preserved in the recombinant protein and that a specific immunoreagent had been obtained. The anti-MOEP19 serum recognized the identical protein spot of approximately 18 Kda, pI 6 on 2-D gels (Fig. 3) that had been cored and microsequenced, as well as a single more acidic MOEP19 isoform of the same mass but shifted by approximately 0.5 pI unit (Fig. 3). This second, acidic spot was microsequenced yielding MOEP19 peptide sequences. This protein microheterogeneity suggested the possibility of a single major post-translational modification of MOEP19 which resulted in the second acidic isoform.

Tissue specificity of MOEP19 at mRNA and protein levels

After 30 cycles of RT PCR performed on 70 ng total RNA isolated from mouse tissues, MOEP19 transcripts were detected only in the ovary, thymus and oocyte samples (Fig. 4) while β-actin amplimers gave similar signals levels in all tissues, indicating input RNAs were equivalent in the samples. This RT-PCR data confirmed the tissue distributions inferred from expressed sequence tags found in the current EST databases. Mouse EST databases currently show MOEP19 EST’s in oocytes, fertilized embryos and thymus; only one EST was reported in pituitary gland.

To examine MOEP19 protein expression in different tissues an extract from 35 mouse oocytes and 50 μg of total protein from different mouse tissues were probed with anti-MOEP19 rat serum by western blot (Suppl. Fig 2). No immunoreactions were detected in tissues other than oocytes. Although mRNA for MOEP19 was noted by PCR (Fig. 4) in thymus, MOEP19 protein was not detected in thymus protein extracts. Immunofluorescence performed on ovary (see below) and thymus sections confirmed the abundance of MOEP19 in the egg cytoplasm in various follicles but did not reveal MOEP19 in any thymic cell type.

In vitro Phosphorylation of MOEP19

Since five potential sites of serine/threonine phosphorylation were predicted in MOEP19, increasing concentrations of recombinant MOEP19 were added to constant amounts of casein kinase II and protein kinase A in an in vitro kinase assay to study MOEP19 phosphorylation. Dose dependent phosphorylation of recombinant MOEP19 (Fig. 5) occurred with both casein kinase II and protein kinase A. In the absence of recombinant MOEP19, bands indicating autophosphorylation of each enzyme were evident (data indicated in the figure). In these reactions, increased phosphorylation of MOEP19 was accompanied by decreased auto-phosphorylation of casein kinase II (Fig. 5).

Immunofluorescence Localization of MOEP19 in Mouse Ovaries and Oocytes

Gonadal ridges, ovaries of adolescent and adult mice—No MOEP19 immunofluorescence was noted in primordial germ cells in sections of gonadal ridges from either male or female day 14 embryos (data not shown). Staining of ovary sections from two-week old adolescent mice revealed MOEP19 immunoreactivity in the ooplasm of oocytes in primary and secondary follicles (Fig. 6). This pattern was compared with the staining pattern of the egg peptidyl arginine de-iminase, ePAD, which stains the oocyte cytoplasm in all follicular stages (Pedersen and Peters, 1968) including primordial follicles (Wright et al, 2003). Paraffin sections of adult mouse ovaries fixed with 4 % PFA were stained with polyclonal anti-MOEP19 or pre-immune rat sera. Anti-MOEP19 serum specifically and selectively stained oocyte cytoplasm at in the adult ovary including primary, secondary and Graafian follicles (Suppl. Fig. 3) while pre-immune sera did not stain the sections. In these 5 μm paraffin sections, the entire ooplasm appeared to be stained uniformly. Taken together these results indicate that the MOEP19 protein is not translated in PGCs and suggests MOEP19 translation is initiated in primary follicles, possibly related to oocyte/granulosa cell interactions during ovarian morphogenesis.

Confocal Imaging the MOEP19 Domain in Immature and Mature Oocytes—Oocytes of various follicular stages were recovered from ovaries, stained for MOEP 19 and examined by confocal microscopy [Fig. 7]. In small, immature oocytes from primary and secondary follicles, MOEP19 protein was present at a low concentration uniformly throughout the cytoplasm. The overall immunofluorescent signal for MOEP19 was lower in oocytes at the earlier stages than in larger oocytes from mature follicles, indicating that the protein accumulates as the oocyte develops. MOEP19 staining in oocytes from mature follicles had a distinct cortical staining pattern with diffuse staining of lesser intensity present in the central peri-nuclear cytoplasm. This cortical rim of MOEP19 staining is referred to as the MOEP19 domain. Thus MOEP19 not only accumulated during oocyte growth and maturation but its pattern of distribution changed becoming concentrated at the oocyte cortex.

Ovulated oocytes—Confocal immunofluorescent microscopy of MOEP19 in live stained ovulated zona-intact oocytes or fixed, non-permeabilized zona-intact eggs revealed a faint MOEP19 signal only in the perivitelline space (data not shown). In fixed, permeabilized zona-intact ovulated oocytes MOEP19 immunofluorescence was faint in the perivitelline space and an intense immunoreactivity was observed in cortical egg cytoplasm (Fig. 8). Optical

sectioning revealed that MOEP19 was prominently concentrated not only at the egg cortex but also within the first polar body where the MOEP19 domain was prominent as a cortical crescent. Control staining with pre-immune serum at the identical concentration as immune serum was negative (Fig. 8).

MOEP19 Domain in Relation to Cortical Granules—Double staining of fixed and permeabilized zona-free oocytes with anti-MOEP 19 and the LCA lectin, which specifically stains cortical granules [Xu et al., 1997, Ducibella T et al., 1988], allowed analysis of the position of the MOEP19 cortical domain relative to the zone of cortical granules, which underlies the microvillar domain (Evans et al, 2000). The green cortical granule signal was predominantly superficial to, and did not overlap with, the MOEP19 domain (Fig. 9). Thus the MOEP19 domain had spherical symmetry deep to the location of zone of cortical granules. The MOEP 19 domain underlay both the microvillar and non-microvillar regions of the oocyte (Fig. 9).

Zygotes and Two Cell Embryos—Zona intact eggs and early embryos (fixed with PFA and permeabilized with Triton X-100) were examined for MOEP19 localization during early embryogenesis (Fig. 10A). MOEP19 localized in a symmetrical rim of cortical cytoplasm in both germinal vesicle and metaphase II eggs as well as in the cortical cytoplasm of the zygote, accompanied by staining in the cytoplasm of both polar bodies. In the two cell embryo, the cortical MOEP19 domain in the apices of blastomeres assumed a dome or crescentric shape, however MOEP19 was excluded from those portions of the blastomeres that were in contact with one another. To insure that this restricted staining was not an artifact of fixation and permeabilization blastomeres were stained with a monoclonal antibody to E-cadherin, which labels apposed surfaces. The regions of blastomeres adhesion were labeled, verifying that the oocytes were permeable to primary antibody and that the MOEP19 staining that was absent from the cytoplasm subjacent to zones of intercellular contact was authentic (data not shown, see calnexin staining in the cytoplasm of 4 cell embryos and E-cadherin staining of morulas below).

Four and Eight Cell Embryos—As cleavage progressed, the MOEP19 domain remained polarized in subsequent stages at the apical cortex of each blastomere. In four cell embryos, for example, (Fig 10A) four crescentric arcs at the apex of each blastomeres were prominent. Dense 0.3 um confocal imaging of MOEP19 domains in 4-cell mouse embryos (Supplemental Figs. 4A, B, C) showed no evidence that the MOEP19 domain was distributed in a greater or lesser degree to different blastomeres. The 0.3 um confocal images of the MOEP10 domains in 4-cell embryos were computationally reconstructed and examined from different angles (Fig. 10B). Variations in the apportionment of the MOEP19 domain in different blastomeres were not apparent although a reduced dimension of the MOEP19 domain in the polar body was evident. In order to insure the concentration of MOEP19 in the blastomere cortex was not an artifact of fixation and permeabilization, immunostaining of 4-cell mouse embryos with anti-calnexin antibody was studied (Suppl. Fig. 5). Cytoplasmic localization of calnexin was observed, including peri-nuclear staining. This demonstrated the full accessibility of the embryo interior to primary antibody. Pronuclear stage zygotes and 4-cell embryos stained with control pre-immune serum showed no immunofluorescence (Suppl. Fig. 6). In the 8 cell embryo, in which compaction is initiated, the MOEP19 domain was again observed prominently in the apical cortex of the blastomeres (Fig. 10A). Comparison of 4 with 8 cell embryos, revealed that the arc length of the MOEP19 domain decreased with each cleavage as cell size diminished.

Morulas—The fourth cleavage results in 16 cell morula embryos and the emergence of the inner cell mass lineage. Most remarkably the MOEP19 domain was present only in the apical

cortex of the peripheral blastomeres of morulae (Suppl. Fig 7 and Fig. 10C). The MOEP19 domain was not detected in inner cell mass cells (which lack an “apical” membrane). Anti-E-cadherin, a marker for intercellular contacts, was used as a control for primary antibody permeability to all regions of the morula cytoplasm. The regions of cell contact between inner cell mass blastomeres were stained with E-cadherin (Fig. 10C) supporting the authenticity of the restricted MOEP19 domain at the cell periphery. To further verify the restricted peripheral MOEP19 staining result in morulae a second, cell permeabilization method, methanol treatment, was employed. Morulas were treated with solutions of gradually increasing concentrations of methanol to avoid embryo lysis and then stained with anti-MOEP19 antibody. The pattern of staining obtained with methanol permeabilized embryos (Suppl Figure 8) was identical to that obtained as in morulas permeabilized with Triton X-100. This confirmed the cortical localization of MOEP19 in early embryos with a second method of permeabilization.

Early Blastocyst—Once the blastocele cavity formed MOEP19 became concentrated in the thin rim of cytoplasm within both mural and polar trophectoderm (Fig. 10A). In a subset of early blastocysts faint staining was also seen in the region of the inner mass cells (8 of 14). The shift from a precisely defined rim of cortical cytoplasm in morulae to staining in the cytoplasm of both trophoblasts and inner cell mass cells was interpreted to represent initiation of protein degradation of MOEP19 in accord with Western blot data indicating that concentrations of MOEP19 decline rapidly in the transition from early to expanded blastocysts [see Figure 11 below and Suppl. Fig. 8].

Expanded Blastocysts—In fully expanded blastocysts MOEP 19 protein was undetectable on Western blots (Fig. 11). Immunofluorescent staining (Fig 9A) was also undetectable in the inner cell mass as well as all mural and polar trophectoderm cells (0/20 blastocysts). Interestingly, a single MOEP19 positive cell persisted in 71% of expanded blastocysts (Suppl. Fig. 9). This MOEP19 positive cell was frequently located at the margin of the mural and polar trophectoderm and is likely the polar body, as its position at the mid-region of the embryonic-abembryonic axis is consistent with the position reported most frequently for this cell (Gardner, 1997: 64% of early blastocysts retain one polar body at the mid-region) In order to test the hypothesis that the single MOEP19 positive cell persisted during subsequent development in a specific lineage, e.g. germ line, blastocysts were cultured after hatching for 2 days to allow spreading using the method of Lopez et al and the embryos were stained for MOEP19 as well as Oct-4, a germ lineage marker. We could easily identify the Oct-4 positive germ cells in the cultures but could find no MOEP19 staining in any cell type in the outgrowth cultures (data not shown). This result suggested that MOEP19 does not persist in a specific lineage in the transition from late blastocyst into later stage embryos..

MOEP19 localization in Oocytes and Embryos from In Vivo Morphogenesis—Because the early embryos described above were obtained following normal fertilization by oviductal flushing and subsequent embryo culture, it was important to study the MOEP19 domain in early embryos that resulted from in vivo fertilization and normal intra-oviductal development. Oviducts were flushed at various intervals following fertilization and early embryos were fixed, permeabilized and studied by confocal immunofluorescent microscopy (Suppl Fig. 10). A restricted pattern of MOEP19 was noted in the cortex of zygotes and the MOEP19 domain subsequently apportioned to the apical cortex of blastomeres in 2, 4, 8 and 16 cell embryos. Importantly, the absence of MOEP19 in inner cell mass blastomeres and its restriction to the apex of peripheral blastomeres of morula stage embryos was observed in embryos that developed in vivo in a pattern identical to that observed in embryos that developed in vitro. The early blastocysts developed in vivo also demonstrated MOEP19 fluorescence in mural and polar trophectoderm.

Oocytes and early embryos stained with pre-immune or with adjuvant alone control sera showed no immunofluorescence at any stage (Suppl Fig. 10, lowerl panel). These controls included both cultured embryos and those harvested from oviducts after normal fertilization.

Western analysis of MOEP19 in early embryogenesis

To compare relative amounts of MOEP19 during early development, extracts of 30 eggs or embryos at each of the GV, M2, PN, 2, 4-8, morula, early and late blastocyst stages were separated and probed on Western blots with anti-MOEP19 serum (Fig. 11). MOEP19 protein concentrations did not visibly change from germinal vesicle through morula stages. However, MOEP19 showed a decrease in the early blastocysts and could not be detected in the late, expanded blastocysts. Interestingly, a higher molecular weight MOEP19 isoform (arrows) was present in M2 through morula stages. These western blot data, together with the immunofluorescent localization of MOEP19 showing stage specific loss of MOEP19 before the expansion of the embryo, suggest that MOEP19 functions during early embryogenesis. The constant amount of MOEP19 in these stages also correlates with the immunofluorescent observation of the restricted MOEP19 cortical domain in blastomeres.

Effect of dis-aggregation and re-association on the MOEP19 domain

To investigate the effect of blastomere dis-aggregation and subsequent re-association on the MOEP19 cortical domain, 4-8 cell embryos were dissociated with a small bore micro-pipette. Some blastomeres were fixed immediately while other single dissociated blastomeres were cultured for 18 hrs to allow re-association. The next day those embryoid bodies that formed from the re-association of blastomeres, as well as individual unassociated blastomeres, were fixed and the localization of MOEP 19 was analyzed by immunofluorescence. Single blastomeres fixed following embryo dissociation showed that a rapid re-localization of the MOEP19 zone to the entire blastomere cortex had occurred (Fig. 12). When blastomeres were subsequently cultured overnight, those that reassociated with one another to form reaggregated embryos underwent repolarization such that the MOEP19 domain was evident only at the apical cortex of blastomeres and was absent in areas of cell contact, similar to the pattern observed in 2 cell through morula stage embryos. However, in individual blastomeres that failed to undergo reassociation, during overnight culture, the MOEP19 domain remained as a spherical cortical pattern of immunofluorescence (Fig. 12).

MOEP19 shows no evidence of translation in eggs or early embryos

Following culture of ovulated eggs and 2 cell embryos in ^{35}S -methionine radioactive label was detected in many protein bands in the Triton soluble extracts of both stages (Fig 13). Although MOEP19 contains six methionine residues and MOEP19 proteins were successfully immunoprecipitated and recovered, (as demonstrated by MOEP19 positive detection on Western blots of the immunoprecipitates), the immunoprecipitated MOEP19 bands showed no evidence of methionine incorporation, despite the incorporation of radiolabel into many other protein bands at both stages. This result indicated that MOEP19 is not synthesized at detectable levels in ovulated eggs or in 2 cell embryos.

Polyribonucleotide homopolymer binding of MOEP19

To test if recombinant and endogenous MOEP19 function as RNA binding proteins a simple RNA binding assay, frequently used to characterize RNA binding properties of other RNA-binding proteins (Brown et al., 1998; Burd et al., 1991), was used. The assay employed poly (C) or poly (U) ribonucleotide homopolymers bound to Sepharose beads. Recombinant MOEP19 protein or egg extracts were incubated with poly (C) or poly(U) agarose beads to assess polynucleotide binding, while other aliquots in a competitive assay were preincubated with free poly(U) for 30 min to bind the RNA binding proteins prior to exposure to the poly

(U) agarose. The beads were washed and proteins bound to the beads were eluted with Laemmli buffer and analyzed by Western blot using polyclonal anti-MOEP19 serum. Both recombinant MOEP19 and endogenous MOEP19 in egg extracts bound ribonucleotide homopolymers [Fig. 14]. Free poly (U) competed with RNA binding sites and decreased binding of recMOEP19 to the beads, indicating that both recombinant MOEP19 and endogenous MOEP19 are RNA binding proteins.

Discussion

The MOEP19 domain: evidence for pre-patterning of oocyte cytoplasm related to apical-basal polarity of blastomeres

Considerable evidence supports the concept that apical-basal polarity appears first in the eight cell mammalian embryo as the steps leading to compaction are initiated (Johnson and McConnell, 2004). Junction-adhesion-molecule 1 is recruitment to cell contact sites predominantly during the first hour after division to the eight-cell stage, earlier than any other tight junctional proteins analysed to date and before E-cadherin adhesion and cell polarization (Thomas et al, 2004). Several studies of the ovulated mouse oocyte and early embryo using monospecific antisera to STAT3, Vg1-RBP, Staufen, Eomes and VegT (Johnson and McConnell, 2004), ePAD (Wright et al, 2003), PARD3, PARD6b, EMK1 and PKCζ (Plusa et al, and 2005,Vinot et al, 2005) revealed no asymmetric distribution of these proteins before compaction.. However, other studies have revealed asymmetries associated with spindle formation. Par-3, which is found throughout the GV-intact oocyte, becomes asymmetrically localized during meiosis, associating with condensing chromosomes, meiotic spindles and within a subdomain of the actin cap overlying the spindle as it forms at the site of polar body emission (Duncan et al 2005). Par6 has been observed to concentrate over the animal pole and to partition to the polar body in meiosis (Gray et al 2004). Par6A was localized to the animal pole cortex overlying the asymmetrically positioned spindle that gives rise to the polar body while αPKC localized within spindle poles and kinetochores (Na et al, 2006). Interestingly, Antczak and van Blerkom (1997) examined leptin and STAT3 in mouse and human oocytes and showed that leptin was concentrated in one portion of the oocyte and showed a polarized distribution at the cell periphery in the two cell embryo, while both proteins showed cortical staining restricted to outer blastomeres in early blastocysts. The present finding of the MOEP19 domain is the basis for proposing a model in which morphogenetic determinants related to blastomere polarity and trophectoderm specification exist in a defined region of the mammalian oocyte cortex and are apportioned in a predictable pattern in the zygote and early embryo.

MOEP19 was chosen for detailed characterization from the mouse oocyte proteome because it was an unknown protein with a predicted KH domain RNA binding motif. RNA gradients in Xenopus eggs show patterns that are related to the animal and vegetal poles and appear to play an important role in subsequent morphogenesis (Ephrussi and D.S. Johnston, 2004; Kloc et al, 2001; King, 2005). If the mammalian oocyte has maintained some aspects of mosaic organization, RNA binding proteins would be predicted to show one or more patterns of unique organization, including asymmetrical or polarized localization, concentration in crescents, or asymmetrical apportionment in blastomeres.

MOEP19 provides a biomarker for a domain of oocyte cortical cytoplasm that is spherically symmetrical and regionally restricted. The MOEP19 domain lies basal to the region of cortical granules, which is immediately beneath the oolemma. The spherically symmetrical, regionally restricted MOEP 19 cortical domain observed within the oocyte cytoplasm persists as a restricted dome of MOEP19 immunofluorescence in the apical cortex of the zygote and in each blastomere of 2 cell through morula stage embryos. The MOEP19 domain is absent, however, in regions of cell contact between blastomeres. These observations suggest pre-patterning of

oocyte cytoplasm and an intrinsic oocyte polarity that expresses itself in the apical-basolateral polarity of blastomeres from the first cleavage onward until early blastocyst.

The MOEP19 domain: evidence for selective apportionment of oocyte cytoplasmic components into trophectoderm cells

Previous evidence that allocation of cells to trophectoderm or inner cell mass lineages depends on molecular organization within the mammalian oocyte has remained controversial. The absence of MOEP19 in inner cell mass cells in morula stage embryos suggests that MOEP19 may have some selective role to play in the trophectoderm lineage. As a biomarker for a restricted domain of oocyte cytoplasm, MOEP 19 provides evidence for selective apportionment of mammalian oocyte cytoplasmic components into trophoectoderm cells in morula stage embryos.

MOEP19 arises in oocytes within primordial follicles and forms a cortical domain during oocyte maturation

MOEP19 protein appears first in the ooplasm of primary follicles. As the oocyte grows in size MOEP19 protein accumulates within the ooplasm. The definitive formation of the cortical MOEP19 domain is related to oocyte size and occurs in large pre-ovulatory follicles through an as yet undefined process of segregation of ooplasm. The MOEP19 domain thus serves as a biomarker of oocyte maturation, although the specific cytoskeletal elements and organelles involved are presently unknown.

MOEP19 is a maternal effect gene

The inability to detect radioactive methionine incorporation into MOEP19 in ovulated oocytes and early embryos suggests that MOEP19 messages are not substantively translated after ovulation or during early embryogenesis. This finding is in accord with the observations that there is a limited pre-formed amount of this protein. MOEP19 is restricted to the apical cortex of the first two blastomeres; and subsequently, the cortical MOEP19 domain is distributed to crescentric domains of decreasing arc in daughter blastomeres. MOEP19 does not insert into the cytoplasmic regions underlying where new baso-lateral membranes are formed following each cleavage. Western blot and immunofluorescent tracing of MOEP19 protein in oocytes and early embryos cultured in vitro support the conclusion that MOEP19 persists in the zygote and embryo through early blastocysts and disappears by the late blastocyst stage from all but a single cell. This single cell is likely the polar body, based upon its location. Taken together the Western blot and immunofluorescence images lead to the hypothesis that at a precise stage of blastocyst development, between day 5-6 in vitro, MOEP19 degradation occurs. Together with the finding that MOEP19 arises during oogenesis in primary follicles, accumulates within the ooplasm during oogenesis, and redistributes prior to ovulation, these observations support the conclusion that *MOEP19* is a maternal effect gene with respect to early embryogenesis.

MOEP19 is the first mammalian KH domain protein to show a molecular mosaicism in the oocyte that is transmitted to blastomeres

Our results show that recombinant and endogenous MOEP19 function as poly-nucleotide binding proteins. MOEP19 contains a KH-domain, which is conserved among RNA-binding proteins including the Fragile X mental retardation gene (FMR1) and neuro-oncological ventral antigen 1 in *Homo sapiens*, *Bicaudal C* in *Drosophila*, and *mex-3*, *gld-1* and gld-3 in *Caenorhabditis elegans* (reviewed in Adinolfi et al. 1999). *MEX-3* is a component of P-granules, germ-line determinants in *C. elegans* (Draper et al. 1996) and gld-3 plays a role in the timing of mitosis in the germline (Eckmann 2004). It is notable that MOEP19 is the first mammalian protein in the RNA-binding superfamily to demonstrate a pattern of molecular mosaicism in the oocyte that is transmitted to blastomeres.

MOEP19 protein expression and Dppa5 [Esg-1]

In the mouse genome database MOEP19's closest relative (25% identity) is currently embryonal stem cell gene 1 [Esg-1] also known as developmental pluripotency protein 5 (Dppa5). The Dppa5/Esg-1 gene was first identified as a pI 3-4, 14 kDa embryonal carcinoma protein that was down regulated by hexamethylenebisacetamide, an inducer of EC differentiation (Astigiano et al 1991). Esg-1 was later confirmed as a specific marker of ES cells that was associated with their pluripotency in an expression array comparison of embryonic stem cells, trophoblast stem cells and mouse embryo fibroblasts (Tanaka et al, 2002). Esg-1 was independently named developmental pluripotency associated protein 5 (Dppa5), based upon the observation that it had an expression pattern in eggs and early embryos similar to Oct-4 [Bortvin, 2003]. The Dppa5 nomenclature is now used in Genbank. Esg-1 expression was found to be extremely low in, or absent from, oocytes and fertilized eggs, but it is strongly induced at the 2-cell stage reaching maximum levels at the 4-cell stage. Esg-1 expression is detectable neither in midgestation embryos nor in neonatal tissues. Antibodies directed against a glutathione S-transferase-esg-1 fusion product detect a protein of M(r) ~14,000 in F9 embryonal carcinoma cells, but not in differentiated cells. In contrast, MOEP 19 is a maternal effect gene transcribed during oogenesis, although both MOEP19 and esg-1 are present in 2 cell through early blastocyst stages.

MOEP19 Tissue Specificity

The preponderance of ESTs for MOEP 19 appear in the oocyte and early embryo. Our results indicate that the messages for MOEP19 are likely not translated at appreciable levels in the ovulated egg or early embryo. Although we confirmed the indication from ESTs that transcription of MOEP19 mRNAs occurred in the mouse thymus, all attempts to detect or localize MOEP19 protein in the thymus by Western blot and immunocytochemistry proved unsuccessful. Thus it is possible the MOEP19 message remains untranslated in the thymus. The single report of a MOEP19 cDNA in adult male pituitary gland (Carninci and Hayashizaki, 1999) also deserves further study.

MOEP19 Phosphorylation and MOEP19 protein microheterogeneity

The protein microheterogeneity of MOEP19 detected on 1 and 2-D western blots of proteins from eggs and early embryos and confirmed by microsequencing indicates that the major isoform of MOEP19 is a protein of 18.5 kDa, pI 5.8. A minor isoform carries slightly more mass, has a pI of approximately 5.2, and potentially represents a phosphorylated form. In vitro phosphorylation of recombinant MOEP19 verified that this protein is a substrate for both casein kinase II and PKA.

Organelles within the MOEP19 domain in the oocyte

The main concentration of MOEP19 is in the MOEP19 domain at the cortex of the oocyte just beneath the zone of cortical granules, which in turn lie immediately beneath the oolemma. The ooplasm immediately deep to the cortical granules in MII oocytes contains a variety of ER cisternae, which are usually devoid of ribosomes and comprise aggregates of small vesicles, large lucent vesicles and tubular extensions of membranes (Fissore et al, 1999). Thus, MOEP19 may associate with the ER, although its precise localization in relation to the ER membranes and lumen and with respect to various ER vesicle types requires ultrastructural study. Interestingly, the ER subcompartment in the cortex of the vegetal pole of Xenopus oocytes where germ cell determinants accumulate has been implicated in the localization of Vg1 RNA by vera protein (Deshler et al, 1997).

Predictions from the MOEP19 Model

Unlike pre-patterning in large invertebrate and lower vertebrate eggs in which asymmetries in molecular organization occur in the animal or vegetal poles following fertilization, the pre-patterning revealed by the MOEP19 domain in the mammalian oocyte appears to represent a simplified, elegant pattern adapted to a smaller, compact oocyte while utilizing common themes previously revealed in invertebrates. The unfertilized murine oocyte is spherically symmetrical with respect to the MOEP 19 domain which confers a pre-patterning related to apical-basolateral polarity that persists in the zygote and subsequent stages through morula. The identification of the MOEP19 domain suggests that the mammalian oocyte shares with invertebrates and lower vertebrate eggs similar fundamental mechanisms of RNA regionalization and a strategy of pre-patterning that employs cortical domains or “crescents” of cytoplasm. The eggs of frogs, tunicates and insects are large and show regionally restricted concentrations of RNAs that migrate to animal or vegetal poles after fertilization. The smaller mammalian oocyte also possesses regionally restricted RNA binding proteins [and by inference RNAs] but differs from these other eggs in: 1) maintenance of a cortical symmetrical localization of the RNA binding protein in the fertilized oocyte; 2) the uniform apportionment of the MOEP19 domain to each blastomeres at first and second cleavage; and 3) the apical polarization of the MOEP19 domain evident at the 2 cell stage onward through morula. It should be noted that other RNA binding proteins may show different localization patterns as their cell biology is studied, while discovery of other proteins that display a MOEP19 pattern in early development would strengthen this model of mammalian oocyte pre-patterning.

The re-positioning of the MOEP19 domain and plasticity of the early embryo

It has long been appreciated that the mammalian embryo has a remarkable capacity for adaptation. Experimental manipulation of the relative positions of cells of the early embryo by the removal, addition, or rearrangement of blastomeres, results in the constituent cells adjusting to their new position and continuing on with development, apparently without resorting to migration back to their former positions. Blastomeres appear to be able to recognize their new relative positions and change their developmental pathways accordingly [Tarkowski and Wroblewska,1967; Hillman et al, 1967; Hogan and Tilly, 1978]. These findings have in the past suggested that mammalian embryos do not rely on a fixed oocytic gradient of morphogens which must be maintained though cleavage if early development is to proceed normally. What mechanisms underlie this capacity for adaptation? How does the embryo direct allocation toward different fates after re-association of blastomeres? The ability of blastomeres to reposition the MOEP19 domain upon dissociation and to re-establish the polarized MOEP19 domain upon re-association may point to a fundamental mechanism of cytoskeletal adaptation and repositioning of RNA binding proteins (and by inference their bound RNAs) that underlies this capacity for adaptation.

Supplementary Material

Refer to Web version on PubMed Central for supplementary material.

Acknowledgements

*The authors would like to thank Dr. Ann Sutherland and Dr. Barry Gumbiner for critical reading of this manuscript. This work was supported by The Kenneth A. Scott Charitable Trust, a Keybank Trust, Ovature Research, a subsidiary of Genetics Savings & Clone, NIH D43 TW/HD 00654 from the Fogarty International Center and National Institutes of Health Grant HD U54 29099.

References

Antczak M, van Blerkom J. Oocyte influences on early development: the regulatory proteins leptin and STAT3 are polarized in mouse and human oocytes and differentially distributed within the cells of the

preimplantation stage embryo. Molecular Human Reproduction 1997;12:1067–1086. [PubMed: 9464852]

Astigiano S, Barkai U, Abarzua P, Tan SC, Harper MI, Shernam MI. Changes in gene expression following exposure of nulli-SCCI murine embryonal carcinoma cells to inducers of differentiation: characterization of a down-regulated mRNA. 1991

Bierbaum P, MacLean-Hunter S, Ehlert F, Moroy T, Muller R. Cloning of embryonal stem cell-specific genes: characterization of the transcriptionally controlled gene esg-1. Cell Growth Differ 1994;5(1): 37–46. [PubMed: 8123591]

Bordier C. Phase separation of integral membrane proteins in Triton X-114 solution. J. Biol. Chem 1981;256:1604–1607. [PubMed: 6257680]

Bortvin A, Eggan K, Skaletsky H, Akutsu H, Berry DL, Yanagimachi R, Page DC, Jaenisch R. Incomplete reactivation of Oct-4 related genes in mouse embryos cloned from somatic nuclei. Development 2003;130:1673–1680. [PubMed: 12620990]

Brown V, Small K, Lakkis L, Feng Y, Gunter C, Wilkinson KD, Warren ST. Purified recombinant Fmrp exhibits selective RNA binding as an intrinsic property of the fragile X mental retardation protein. J. Biol. Chem 1998;273:15521–1552. [PubMed: 9624140]

Burd CG, Matunis EL, Dreyfuss G. The multiple RNA-binding domains of the mRNA poly(A)-binding protein have different RNA-binding activities. Mol. Cell Biol 1991;11:3419–3424. [PubMed: 1675426]

Carninci P, Hayashizaki Y. High-efficiency full-length cDNA cloning. Meth. Enzymol 1999;303:19–44. [PubMed: 10349636]

Conklin GE. The organization and cell lineage of the ascidian egg. J. Acad. Nat. Sci. Phila 1905;13:1–119.

Conklin GE. Mosaic development in ascidian eggs. J. Exp. Zool 1905;2:145–223.

Ducibella T, Rangarajan S, Anderson E. The development of mouse oocyte cortical reaction competence is accompanied by major changes in cortical vesicles and not cortical granule depth. Dev.Biol 1988;130:789–92. [PubMed: 3197932]

Deshler JO, Highett MI, Highett, Schnapp BJ. Localization of Xenopus Vg1 mRNA by Vera protein and the endoplasmic reticulum. Science 1997;276:5315, 1128–1131.

Duncan FE, Moss SB, Schultz RM, Williams C,J. PAR-3 defines a central subdomain of the cortical actin cap in mouse eggs. Dev. Biol 2005;280(1):38–47. [PubMed: 15766746]

Eckmann CR, Crittenden SL, Suh N, Kimble J. GLD-3 and control of the mitosis/meiosis decision in the germline of Caenorhabditis elegans. Genetics 2004;168:147–160. [PubMed: 15454534]

Ephrussi A, Johnston DS. Seeing is believing: the bicoid morhogen gradient matures. Cell 2004;116:143–152. [PubMed: 14744427]

Evans JP, Foster JA, McAvery BA, Gerton GA, Kopf GS, Schultz RM. Effects of perturbation of cell polarity on molecular markers of sperm-egg binding sites on mouse eggs. Biol. Reprod 2000;62:76–84. [PubMed: 10611070]

Fissore RA, Longo FJ, Anderson E, Parys JB, Ducibella T. Differential distribution of inositol trisphosphate receptor isoforms in mouse oocytes. Biology of Reproduction 1999;60:49–57. [PubMed: 9858485]

Filipenko NR, MacLeod TJ, Yoon CS, Waisman DM. Annexin A2 is a novel RNA-binding protein. J.Biol.Chem 2004;279:8723–8731. [PubMed: 14672933]

Fleming TP, Sheth B, Fesenko I. Cell adhesion in the preimplantation mammalian embryo and its role in trophectoderm differentiation and blastocysts morphogenesis. Front. Biosci 2001;6:D1000–D1007. [PubMed: 11487467]

Gardner RL. Can developmentally significant spatial patterning of the egg be discounted in mammals? Human Reproduction Update 1996;2:3–27. [PubMed: 9079400]

Gardner RL. The early blastocysts is bilaterally symmetrical and its axis of symmetry is aligned with the animal-vegetal axis of the zygote in the mouse. Development 1997;124:289–301. [PubMed: 9053306]

Gardner, RL.; Davies, TJ. Mouse chimeras and the analysis of development. In: Tuan, RS.; Lo, C., editors. Developmental Biology Protocols. Human Press; Totowa, New Jersey: 2000. p. 397-424.

Gardner RL. Specification of embryonic axes begins before cleavage in normal mouse development. Development 2001;128:839–847. [PubMed: 11222139]

Gardner RL. Experimental analysis of second cleavage in the mouse. Human Reproduction 2002;17:3178–3189. [PubMed: 12456621]

Gardner RL. The case for pre-patterning in mammals. Birth Defects Res., Part C, Embryology Today 2005;75:142–150.

Gardner RL, Davies TJ. An investigation of the origin and significance of bilateral symmetry of the pronuclear zygote in the mouse. Human Reproduction 2006;21(2):492–502. [PubMed: 16210387]

Grey D, Plusa B, Piotrowska K, Na J, Tom B, Glover DM, Zernicka-Goetz M. First cleavage of the mouse embryo responds to change in egg shape at fertilization. Current Biology 2004;14:397–405. [PubMed: 15028215]

Guan K, Nayernia K, Wagner S, Dressel R, Lee JH, Nolte J, Wolf F, Li M, Engel W, Hasenfuss G. Pluripotency of spermatogonical stem cells from adult mouse testis. Nature. 2006

Hiragi T, Solter D. First cleavage plane of the mouse egg is not pre-determined but defined by the topology of the two apposing pronuclei. Nature 2004;430:360–364. [PubMed: 15254539]

Johnson MH. Axes in the egg? Curr Biol 2001;11:R281–R284. [PubMed: 11413020]7

Johnson MH, McConnell JML. Lineage allocation and cell polarity during mouse embryogenesis. Seminars in Cell and Developmental Biology 2004;15(5):583–597. [PubMed: 15271304]

Katayama S, Tomaru Y, Kasukawa T, Waki K, Nakanishi M, Nakamura M, Nishida H, Yap CC, Suzuki M, Kawai J, Suzuki H, Carninci P, Hayashizaki Y, Wells C, Frith M, Ravasi T, Pang KC, Hallinan J, Mattick J, Hume DA, Lipovich L, Batalov S, Engstrom PG, Mizuno Y, Faghihi MA, Sandelin A, Chalk AM, Mottagui-Tabar S, Liang Z, Lenhard B, Wahlestedt C. Antisense transcription in the mammalian transcriptome. Science 2005;309(5740):1564–1566. [PubMed: 16141073]

King ML, Messitt TJ, Mowry KL. Putting RNAs in the right place at the right time: RNA localization in the frog oocyte. Biology of the Cell 2005;97(1):19–33. [PubMed: 15601255]

Kloc M, Bilinski S, Cahn A, Allen L, Zerafoss N, Etkin L. RNA localisation and germ cell determination in Xenopus. Int Rev Cytol 2001;203:63–91. [PubMed: 11131528]

Kurotaki Y, Hatta K, Nakao K, Nabeshima Y, Fujimori T. Blastocyst Axis Is Specified Independently of Early Cell Lineage But Aligns with the ZP Shape. Science 2007;316:719–723. [PubMed: 17446354]

Laemmli UK. Cleavage of structural proteins during the assembly of the head of bacteriophage T4. Nature 1970;227:680–685. [PubMed: 5432063]

Louvet-Vallee S, Vinot S, Maro B. Mitotic spindles and cleavage planes are oritneted randomly in the two-cell mouse embryo. Current Biology 2005;15:464–469. [PubMed: 15753042]

Madera M, Vogel C, Kummerfeld SK, Chothia C, Gough J. The SUPERFAMILY database in 2004: additions and improvements. Nucl. Acids Res 2004;32:D235–D239. [PubMed: 14681402]

Na J, Zernicka-Goetz M. Asymmetric Positioning and Organization of the Meiotic Spindle of Mouse Oocytes Requires CDC42 Function. Currrent Biology 2006;16(12):1249–1254.

Nishida H. Localization of egg cytoplasm that promotes differentiation to epidermis in embryos of the ascidian Halocynthia roretzi. Development 1994;120:235–243.

Nusslein-Volhard C. Determination of the embryonic axes of Drosophila. Development Supplement 1991;1:1–10. [PubMed: 1742496]1991

Nishida H. Cell lineage analysis in ascidian embryos by intracellular injection of a tracer enzyme. III. Up to the tissue restricted stage. Dev. Biol 1987;121:526–541. [PubMed: 3582738]

Nishida H. Determination of developmental fates of blastomers in ascidian embryos. Dev. Growth Differ 1992;34:253–262.

Pedersen T, Peters H. Proposal for a classification of oocytes and follicles in the mouse ovary. J. Reprod. Fert 1968;17:555–557.

Piotrowska-Nitsche K, Zernicka-Goetz M. Spatial arrangement of individual 4-cell stage blastomeres and the order in which they are generated correlate with blastocyst pattern in the mouse embryo. Mechanisms of Development 2005;122(4):487–500. [PubMed: 15804563]

Plusa B, Frankenberg S, Chalmers A, Hadjantonakis A, Moore CA, Papalopulu N, Papaioannou VE, Glover DM, Zernicka-Goetz M. Downregulation of Par3 and aPKC function directs cells towards

the ICM in the preimplantation mouse embryo. J Cell Science 2005;118:505–515. [PubMed: 15657073]

Ramalho-Santos M, Yoon S, Matsuzaki Y, Mulligan RC, Melton DA. 'Stemness': transcriptional profiling of embryonic and adult stem cells. Science 2002;298:597–600. [PubMed: 12228720]

Rossant J. Postimplantation development of blastomeres isolated from 4- and 8-cell mouse eggs. J. Embryol. Exp. Morphology 1976;36:283–290.

Rossant J, Tam PPL. Emerging asymmetry and embryonic patterning in early mouse development. Developmental Cell 2004;7(2):155–164. [PubMed: 15296713]

Siomi H, Choi M, Siomi MC, Nussbaum RL, Dreyfuss G. Essential role for KH domains in RNA binding: impaired RNA binding by a mutation in the KH domain of FMR1 that causes fragile X syndrome. Cell 1994;77:33–39. [PubMed: 8156595]

Swalla BJ, Jefferey WR. A maternal RNA localized in the yellow crescent is segregated to the larval muscle cells during ascidian development. Dev. Biol 1995;170:353–364. [PubMed: 7544307]

Tanaka TS, Kunath T, Kimber WL, Jaradat SA, Stagg CA, Usuda M, Yokota T, Niwa H, Rossant J, Ko MSH. Gene expression profiling of embryo-derived stem cells reveals candidate genes associated with pluripotency and lineage specificity genome research. Genome Research 2002;12:1921–1928. [PubMed: 12466296]

Tarkowski AK. Experiments on the development of isolated blastomeres of mouse eggs. Nature 1959;184:1286–1287. [PubMed: 13836947]

Tarkowski AK. Mouse chimeras developed from fused eggs. Nature 1961;190:857–860. [PubMed: 13775333]

Tarkowski AK, Wroblewska J. Development of blastomeres of mouse eggs isolated at the 4- and 8-cell stage. J. Embroyol. Exp. Morphology 1967;18:155–180.

Tarkowski AK, Ozdzenski W, Czolowska R. How many blastomeres of the 4-cell embryo contribute cells to the mouse body? International Journal of Developmental Biology 2001;45(7):811–6. [PubMed: 11732840]

Thomas FC, Sheth B, Eckert JJ, Bazzoni G 3, Dejana E, Fleming TP. Contribution of JAM-1 to epithelial differentiation and tight-junction biogenesis in the mouse preimplantation embryo. Journal of Cell Science 2004;117:5599–5608. [PubMed: 15494378]

Torres-Padilla ME, Parfitt DE, Kouzarides T, Zernicka-Goetz M. Histone arginine methylation regulates pluripotency in the early mouse embryo. Nature 2007;445:214–218. [PubMed: 17215844]

Vinot S, Le T, Ohno S, Pawson T, Maro B, Louvet-Vallée S. Asymmetric distribution of PAR proteins in the mouse embryo begins at the 8-cell stage during compaction. Dev. Biol 2005;282(2):307–319. [PubMed: 15950600]

Wright PA, Bolling LC, Calvert ME, Sarmento OF, Berkeley EV, Shea MC, Hao Z, Jayes FC, Bush LA, Shetty J, Shore AN, Reddi P, Tung KSK, Samy E, Allietta MM, Sherman NE, Herr JC, Coonrod SA. ePAD, an oocyte and early embryo-abundant peptidylarginine deiminase-like protein which localizes to egg cytoplasmic sheets. Dev. Biol 2003;256:73–88. [PubMed: 12654293]

Xu Z, Abbott A, Kopf GS, Schultz RM, Ducibella T. Spontaneous activation of ovulated mouse eggs: time-dependent effects on M-phase exit, cortical granule exocytosis, maternal messenger ribonucleic acid recruitment, and inositol 1,4,5-triphosphate sensitivity. Biol. Reprod 1997;57:743–750. [PubMed: 9314575]

Zernicka-Goetz M. Fertile offspring derived from mammalian eggs lacking either animal or vegetal poles. Development 1998;125:4803–4808. [PubMed: 9806928]

Zernicka-Goetz M. Cleavage pattern and emerging asymmetry of the mouse embryo. Nature Reviews Molecular Cell Biology 2005;6:919–928.

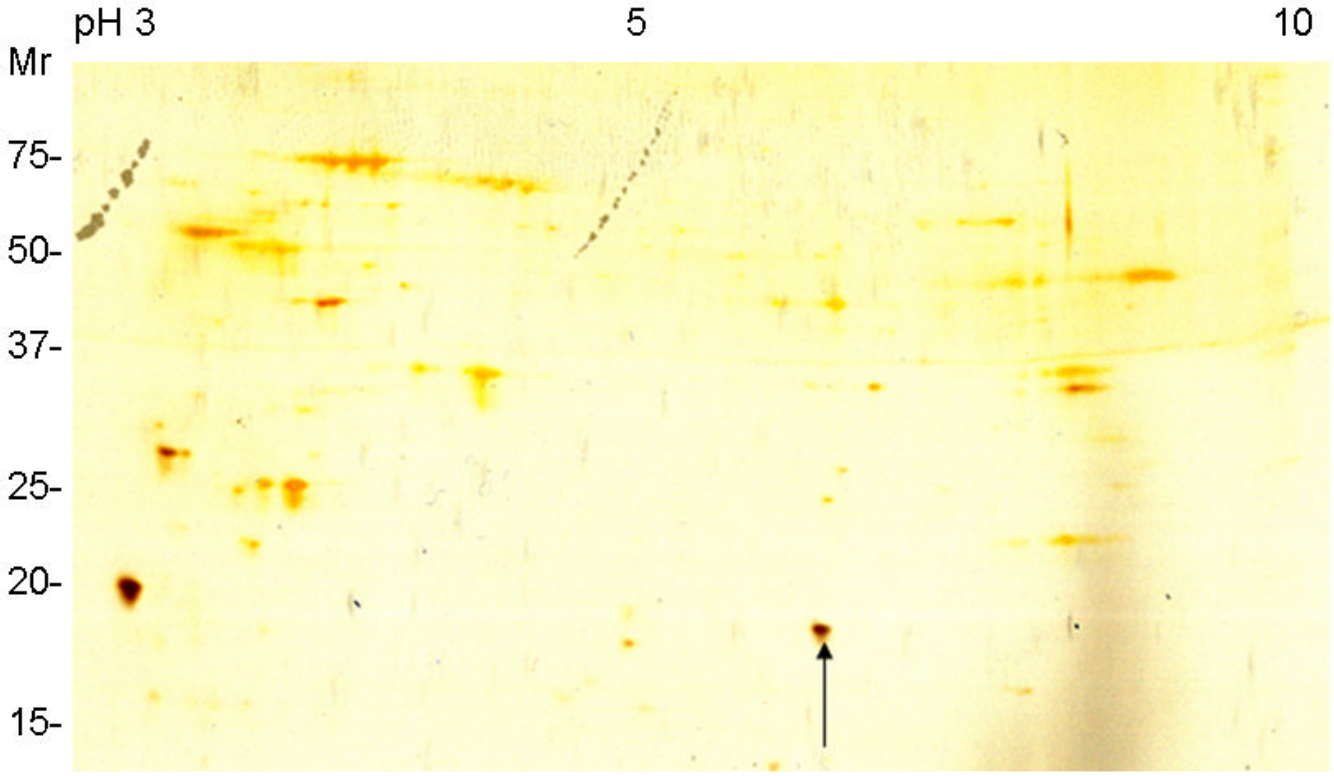

MASHTADADAKPDSDSQKLLNVLPVSLRLRTRPWWFPIQEVS
NPLVLYMEAWVAERVIGTDQAEISEIEWMCQALLTVDSVNSNL
AEITIFGQPSAQTRMKNILLNMAAWHKENELQRAVKVKEVEEF
LKIRASSILSKLSKKGLKLAGFPLPLEGRETQMES

Fig. 1.

Silver stained 2-D gel of hydrophobic proteins obtained by phase partitioning Triton X-114 soluble proteins from 800 zona free mouse oocytes. Proteins were separated using IPG strips (pH 3-10 non-linear) and a Criterion gel system (8-16 % acrylamide gradient). Abundant spots were excised from the gel and microsequenced including the 18.5 Kda, pI 5.8 MOEP19 protein spot identified at the arrow. Upon database searching the peptide microsequences [underlined] obtained from this spot by tandem mass spectrometry matched five peptides contained in a 164 aa hypothetical protein sequence encoded by RIKEN cDNA sequence NM_026480.

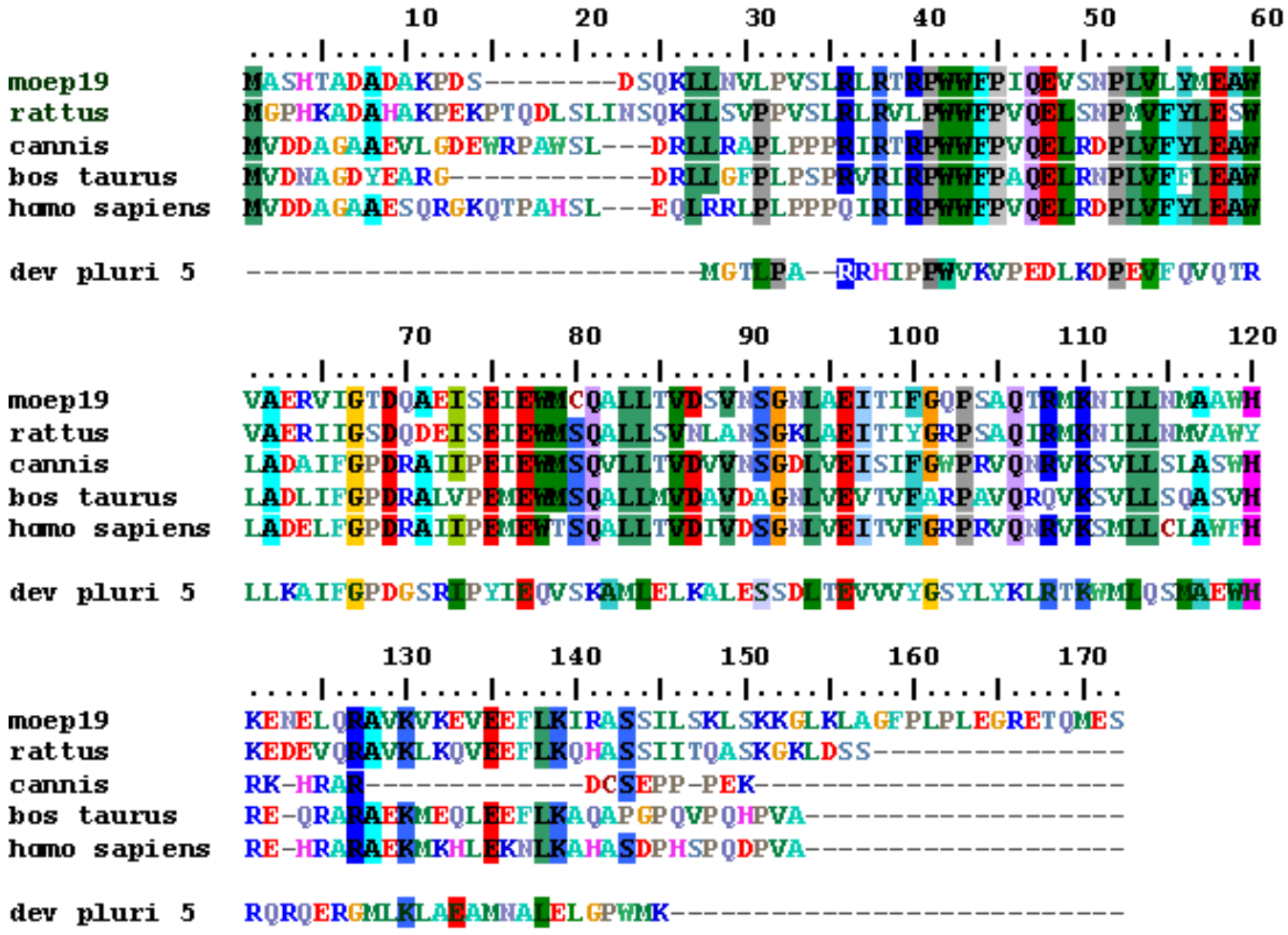

Fig. 2.

Allignment of murine MOEP19 with orthologs from various species and with development pluripotency associated protein 5 [Dppa5/Esg-1]. Each of these proteins contain a predicted RNA binding KH superfamily motif that extends in MOEP19 from aa 40-150.

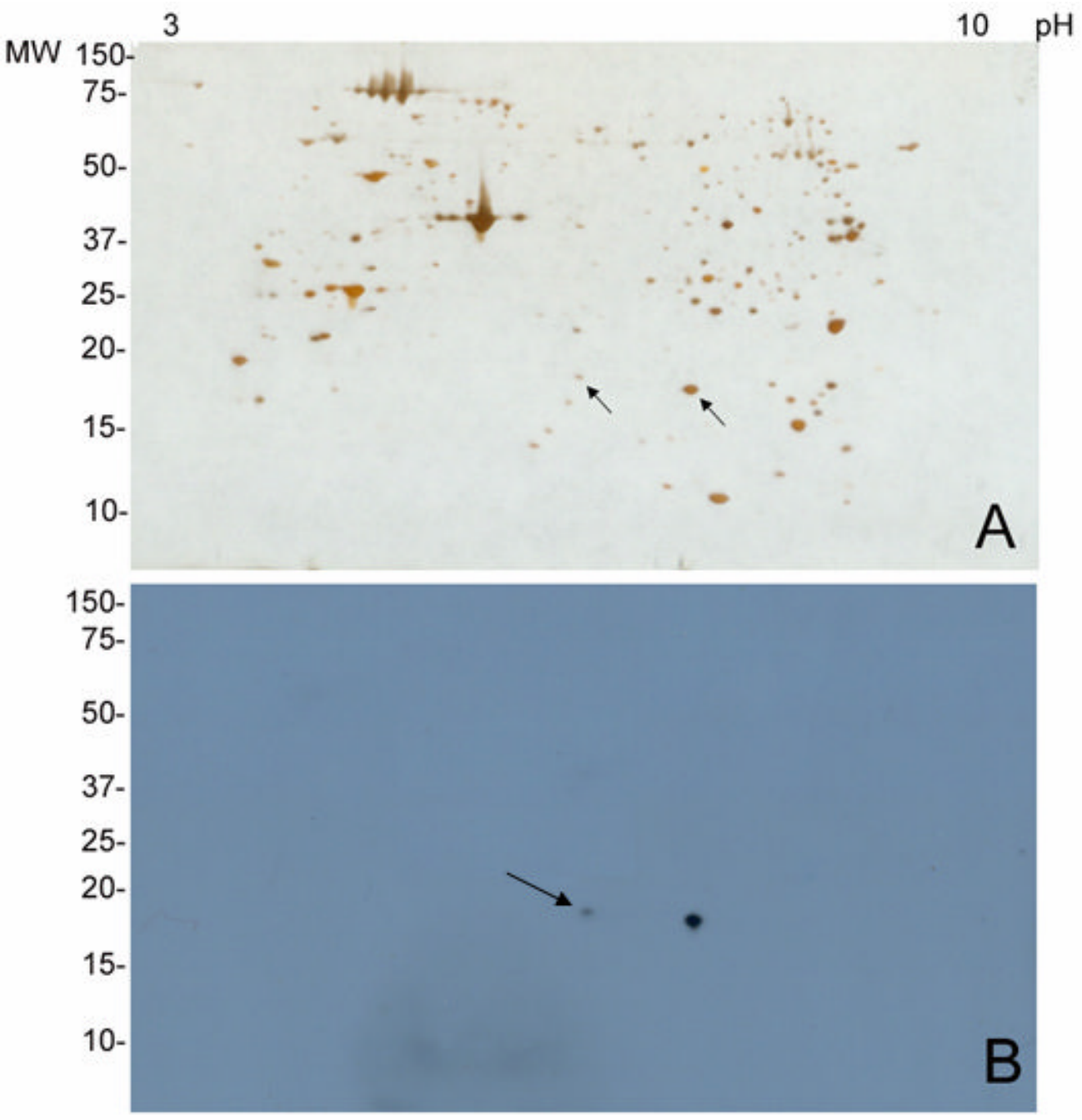

Fig 3.

Proteins from 750 mouse oocytes separated by 2D gel electrophoresis and reacted with anti-MOEP19 serum. A: sliver stained; B: Western blot with anti MOEP19 rat serum revealed two spots. The most intense spot [right] had the same molecular weight [18.5 kDa] and pI [5.8] as the spot originally cored [Fig 1] while the left spot (arrow) gave evidence of a slight increase in mass and was shifted approximately 0.5 pI units to the acidic side.

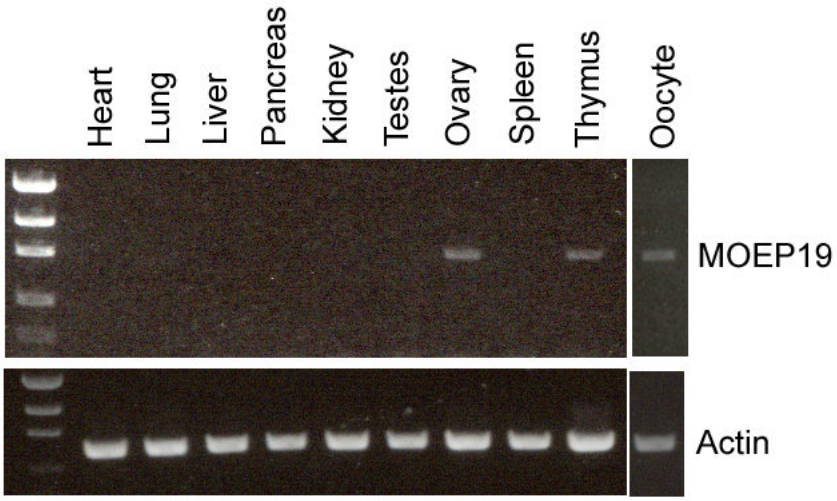

Fig. 4.

Multi-Tissue RT-PCR with MOEP19 or β-actin primers. 70 ng RNA from various mouse tissues was used to amplify MOEP19 and β-actin, which served as a positive control for equal RNA loads in each sample. MOEP19 cDNA was amplified only in ovary, thymus and oocyte RNA samples..

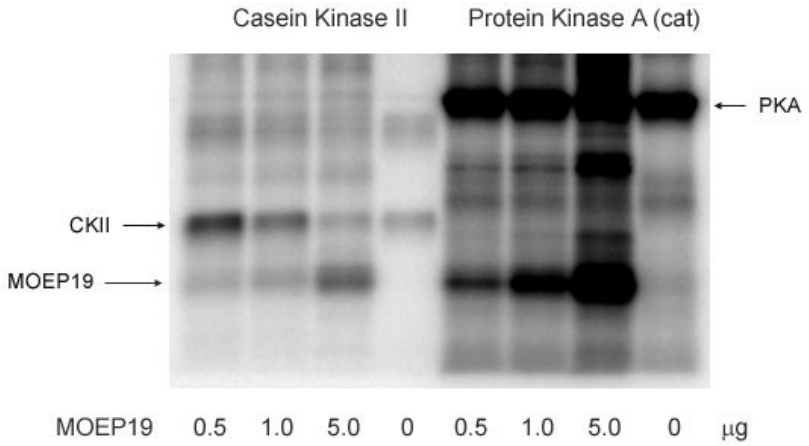

Fig. 5.

Autoradiograph of reaction mixtures following *in vitro* phosphorylation of recombinant MOEP19 with casein kinase II and PKA. Dose dependent phosphorylation of recombinant MOEP19 by both enzymes confirmed the presence of phosphorylation sites for CKII and PKA. In the absence of recombinant MOEP19 only bands indicating auto-phosphorylation of each enzyme were noted. Increased phosphorylation of MOEP19 was accompanied by decreased auto-phosphorylation of casein kinase II.

Fig. 6.

Immunolocalization of MOEP19 and ePAD during oogenesis.. Brightfield phase image of paraffin sections (A) of 2 week old ovaries showing a large oocyte in a multilaminar secondary follicle (S) and clusters of primordial (Pr) oocytes., the majority of which are positive for ePAD (C) a protein which localizes to the cytoskeletal sheets (Wright et al, 2003). Ooplasm within the primordial oocytes was not immunoreactive for MOEP19 (B),.

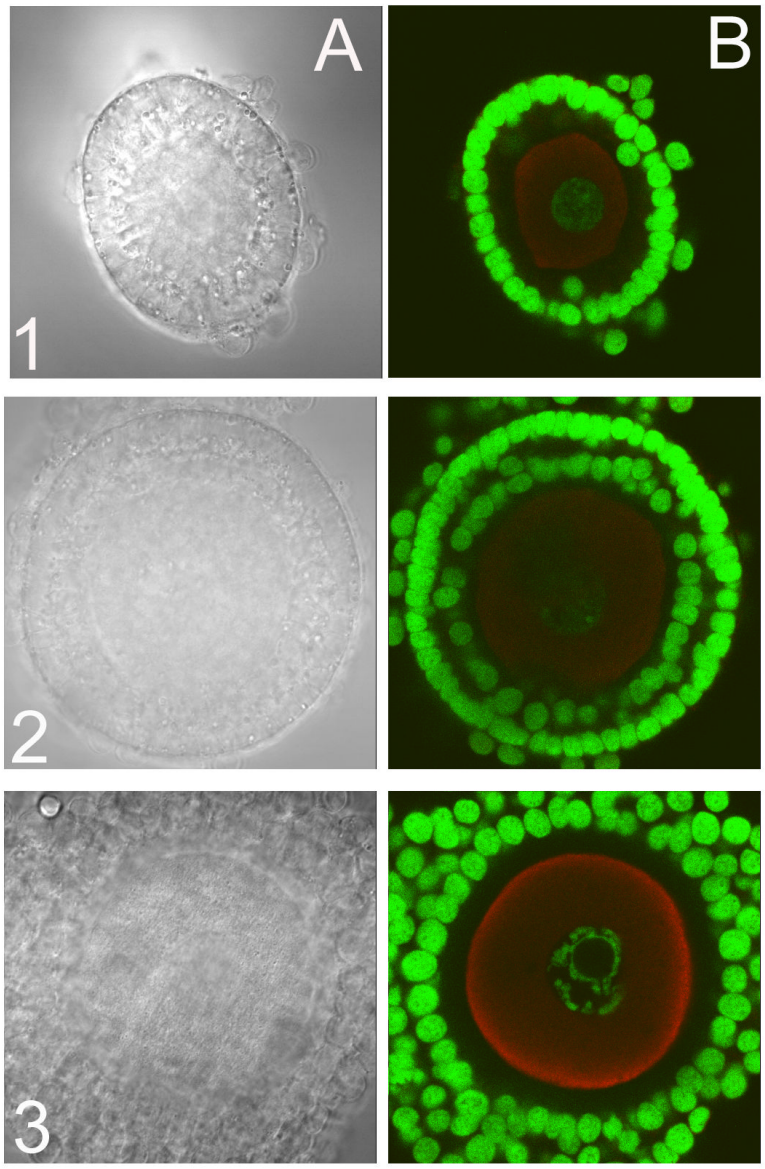

Fig. 7.

Confocal optical sections of MOEP19 staining in mouse oocytes obtained from ovarian follicles at various stages of maturation. A: phase; B: Merge images of MOEP-19 localization with Texas Red and Sytox (green) nuclear staining. Oocytes from primary follicle (1), secondary follicle (2) and antral follicle (3). The smaller immature oocytes show a uniform staining for MOEP19 across the ooplasm. MOEP19 increases in concentration with oocyte maturation and redistributes to the oocyte cortex in oocytes from antral follicles.

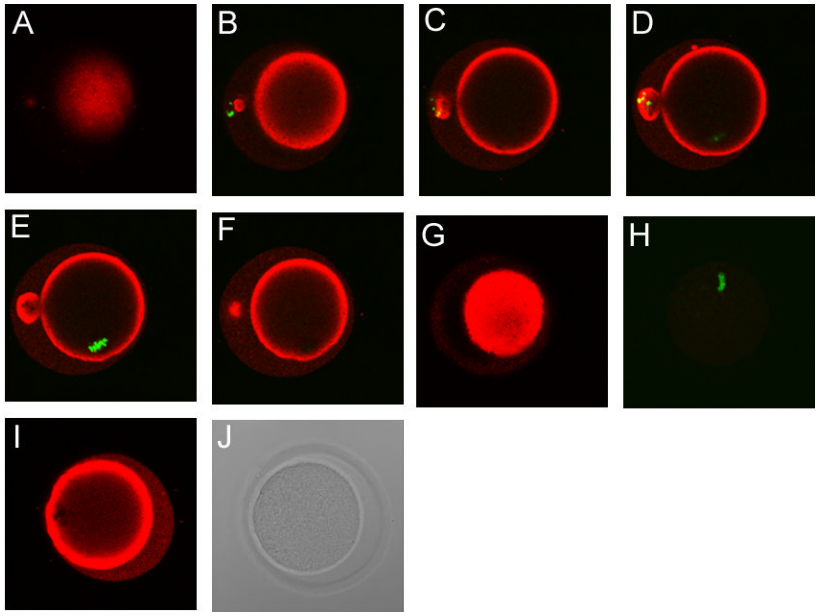

Fig. 8.

Confocal optical sections of MOEP19 immunofluorescence in zona intact permeabilized oocytes. MOEP19 = red, DNA = green. Oocytes were fixed with 4% PFA and permeabilized with 0.5 % Triton X-100. The MOEP19 protein localized to a symmetrical cortical domain in the ooplasm just beneath the oolemma with faint staining persisting in the peri-vittelline space in a zona intact oocyte (A-G). Staining another oocyte with pre-immune serum (H) was negative. Fluorescent confocal image of another oocyte demonstrates a slightly thicker MOEP19 cortical domain (I) as well as faint staining in the peri-vitelline space. Phase image of I shown in J.

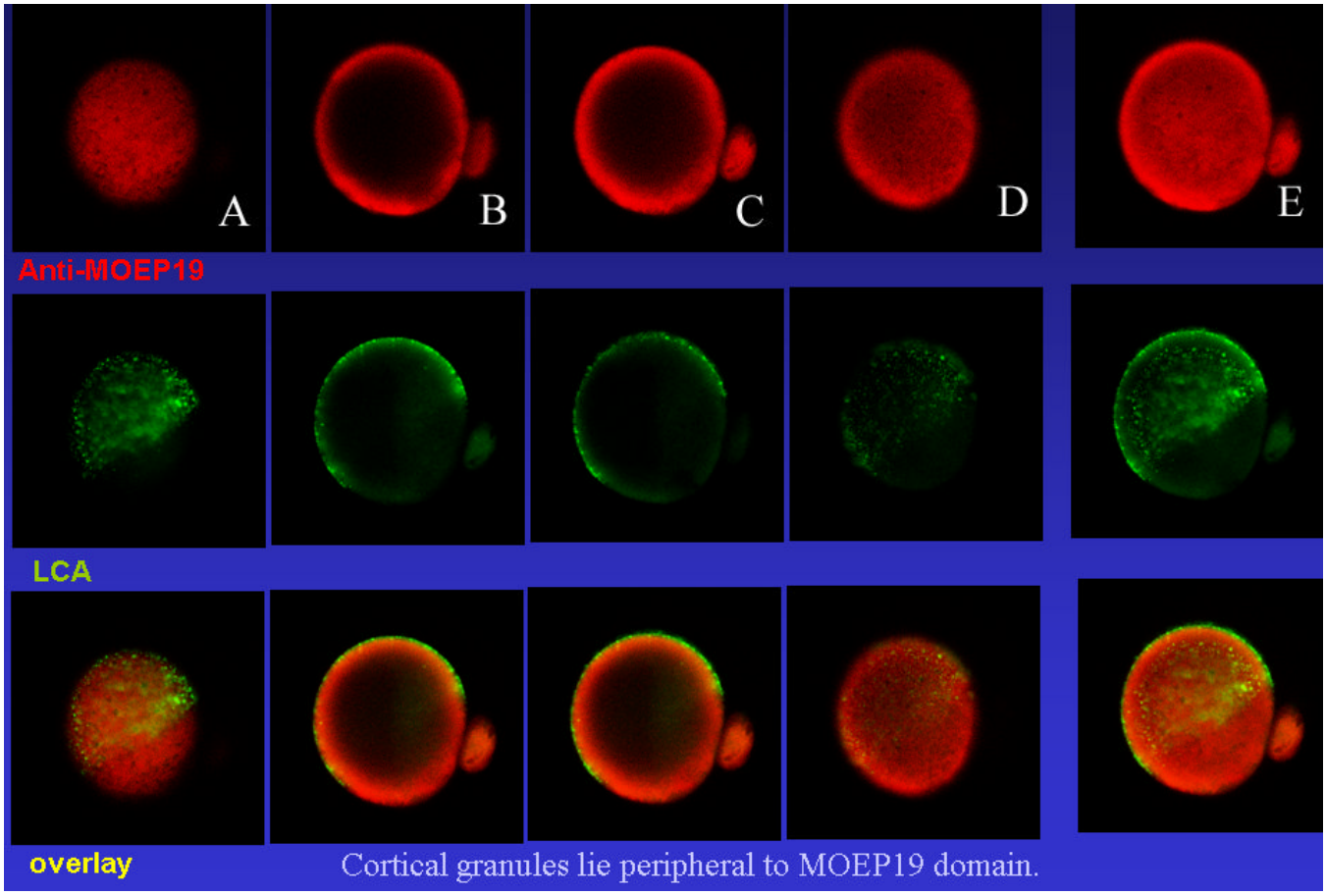

Fig. 9.

A-D Confocal optical sections of a zona-free mouse egg double stained with anti-MOEP19 (red) and LCA lectin (green) which stains cortical granules. E. Merged images of A-D. Yellow signals indicating co-localization of the MOEP19 domain with the zone of cortical granules were not evident in any optical section. The spherically symmetrical MOEP19 domain underlies and is basilar to the zone of cortical granules. In the merged image E, cortical granules form a cap like region known to co-localize with the microvillar domain of the oolemma.

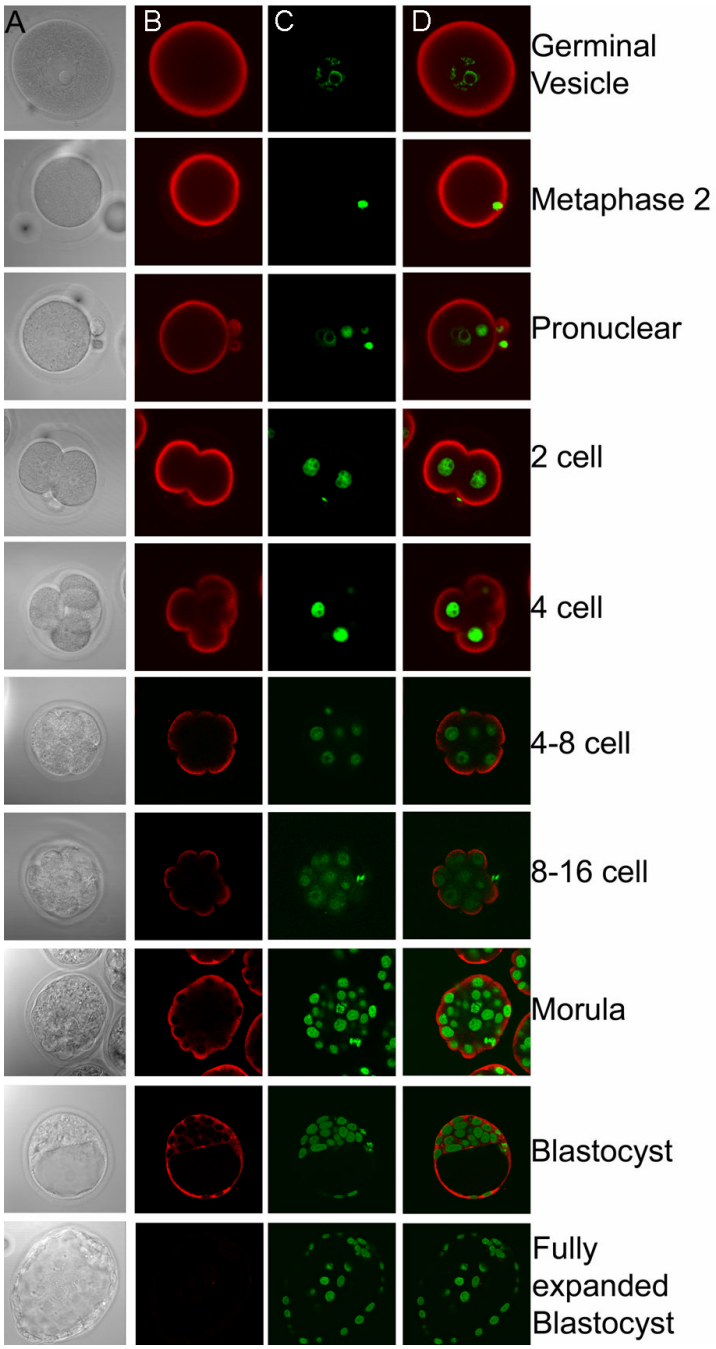

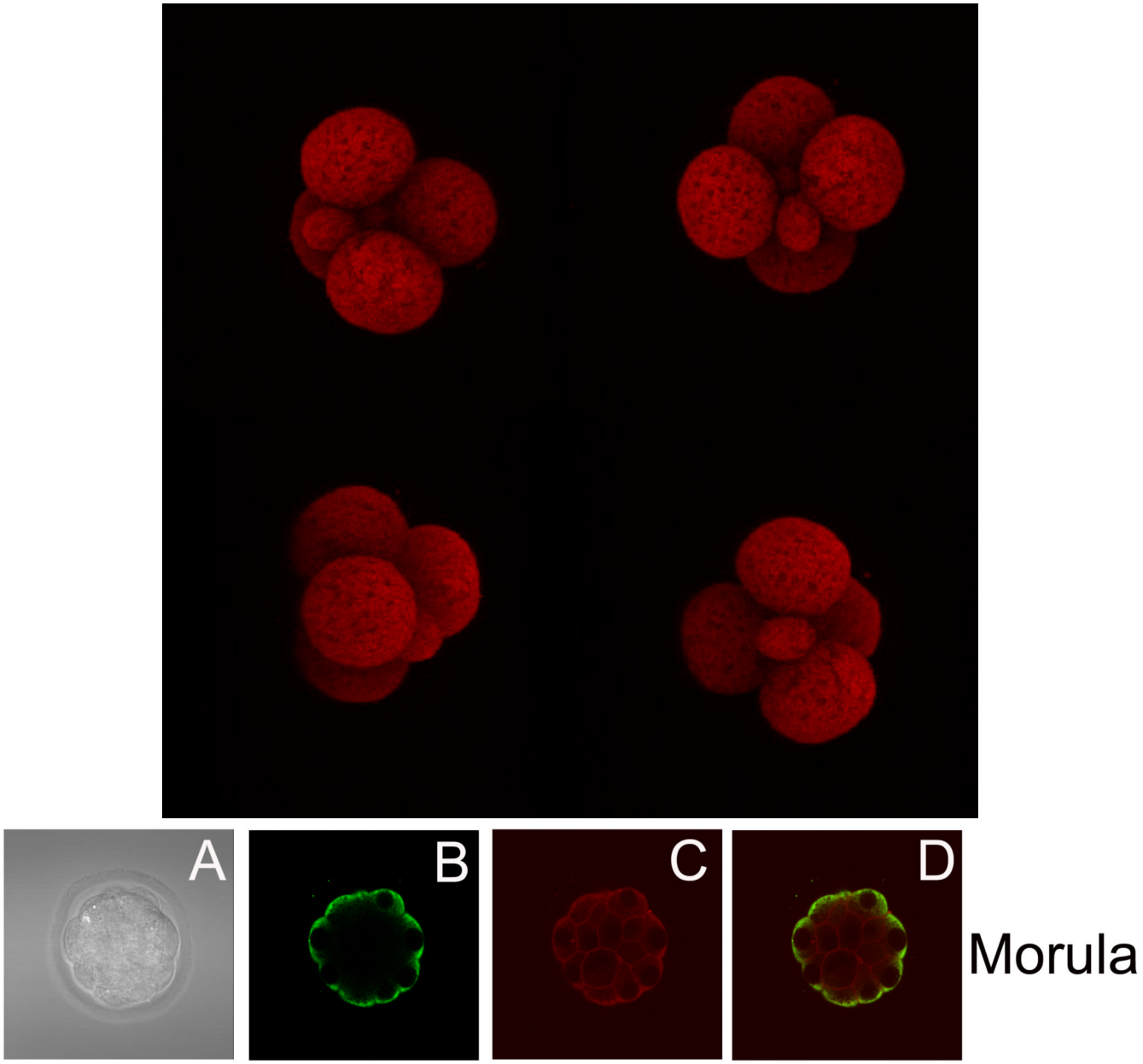

Fig. 10.

Panel A Confocal optical sections of oocytes and cultured early embryos stained with anti-MOEP19 serum. MOEP19 localized to the cortical cytoplasm of the mature egg, zygote and retained a cortical location at the apex of blastomeres through morula stage, while MOEP19 was absent from areas of cell contact between blastomeres. In morula, MOEP19 was restricted to outer blastomeres. Diffuse staining in both mural and polar trophectoderm as well as inner cell mass was observed in early blastocysts. Late blastocysts showed an absence of MOEP19 immunofluorescence. Column A: phase; B: anti-MOEP19; C: Sytox nuclear stain; D: merged image of B&D. Panel B. Computational reconstruction of the MOEP19 domain from 0.3 um confocal images of a 4-cell mouse embryo at different angles of view. Panel C. Morula embryo in phase (A) and stained with anti-MOEP (B, green) or anti-e-cadherin (C, red) including merged image (D) of B & C. The e-cadherin antibody stained zones of intercellular adhesion

between blastomeres in contrast to the restricted domain of MOEP19 at the apex of only outer blastomeres.

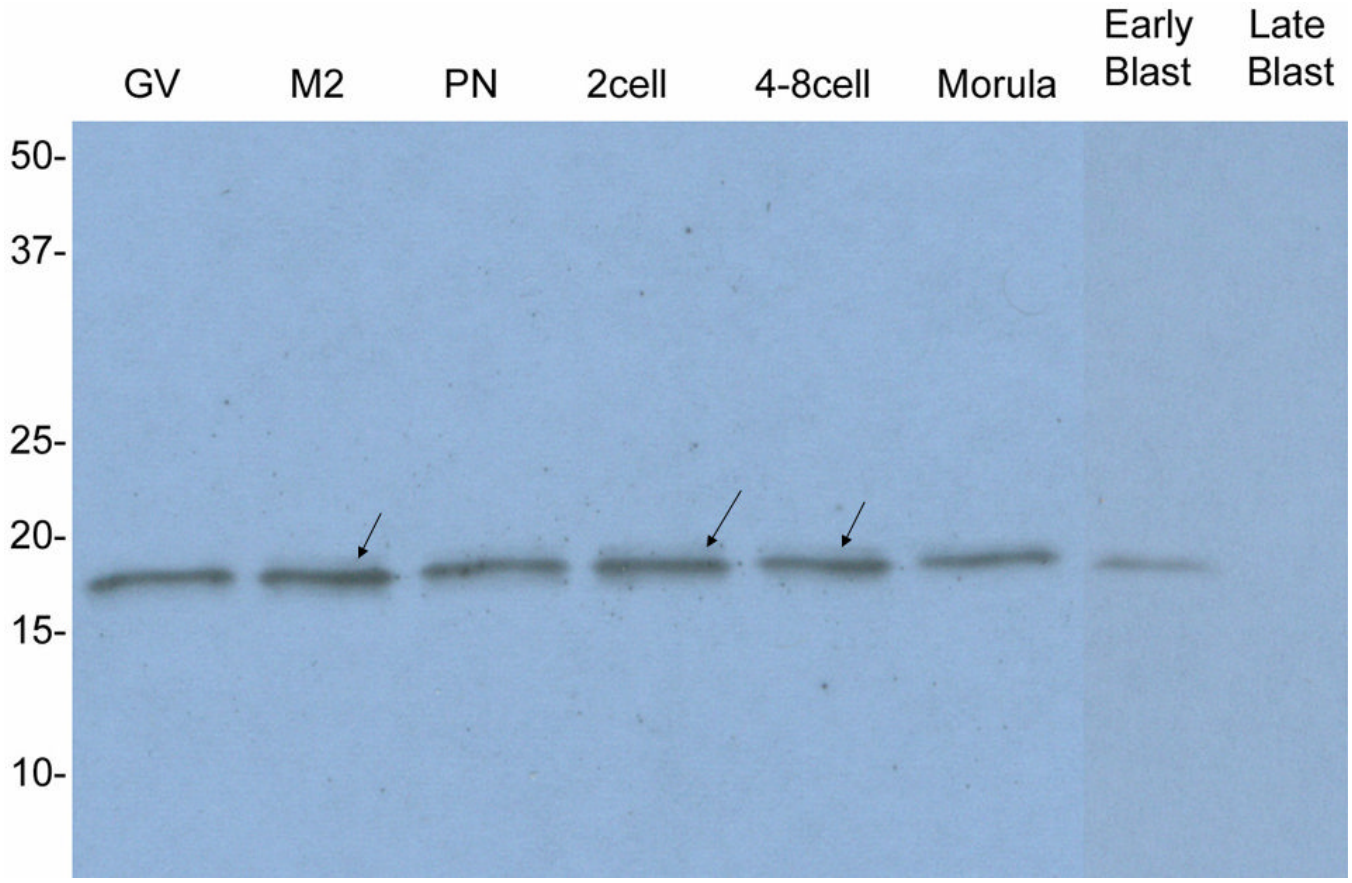

Figure 11.

Relative concentrations of MOEP19 protein in eggs and early embryos assayed by Western Blot. Protein extracts from 30 eggs and embryos at each developmental stage were separated by 1-D SDS PAGE and probed with anti-MOEP19 serum. MOEP19 concentrations did not change from germinal vesicle through morula stage, but decreased in early blastocysts and were undetectable in expanded late blastocysts. A second MEOP19 isoform of slightly higher mass [arrows] was detected in M2 through morula stages.

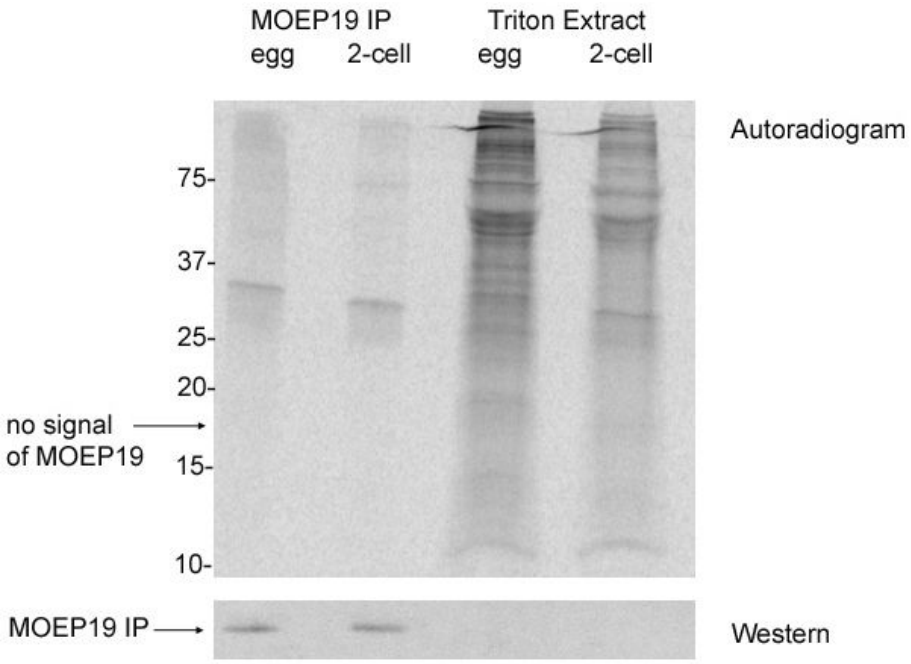

Fig. 12.

MOEP19 immunofluorescence of disaggregated blastomeres from 4-8 cell embryos fixed immediately after dissociation (A-D) or fixed after 16 hours of culture (E-H). Soon after dissociation the MOEP19 domain reassembled as a uniform spherical domain near the periphery of the entire isolated blastomere (A & B). The few blastomeres that did not separate (white arrow) showed a lack of MOEP19 staining at the persisting sites of cell contact (C & D). After 16 hours of culture, embryoid bodies that reassembled from single blastomeres (E & F) repolarized with respect to the MOEP19 domain, while blastomeres that remained isolated demonstrated the spherically symmetrical MOEP19 domain (G & H).

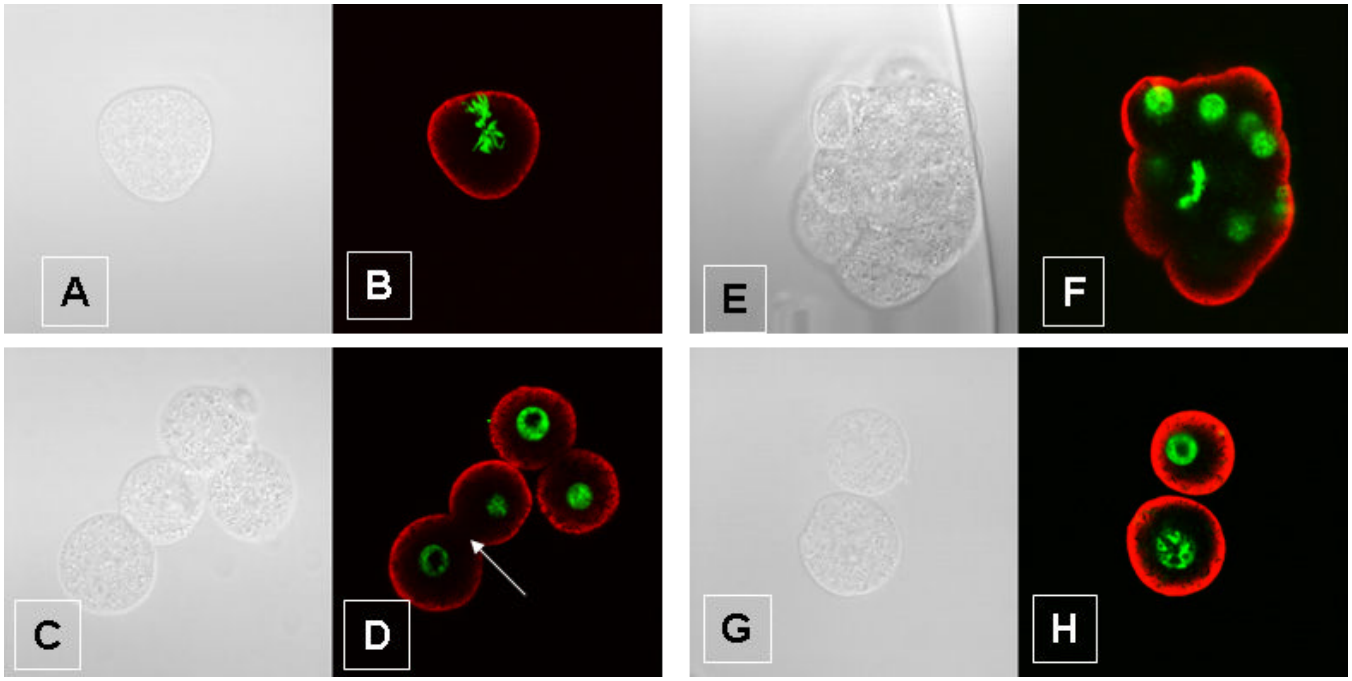

Fig. 13.

Immunoprecipitation of MOEP 19 following ^{35}S-methionine incorporation into newly synthesized proteins of superovulated mouse eggs and two cell embryos. 100 oocytes and 100 2 cell embryos were labeled in culture for 2 hours, oocyte proteins were extracted in 0.5 % Triton X-100 and MOEP19 was immuno-precipitated from the extracts with rat anti MOEP19 serum and Protein-G agarose. The ^{35}S labeled egg and embryo extracts as well as the proteins immunoprecipitated from the extracts were analyzed on an 18 % acrylamide gel, the gel was dried and exposed to a phosphoimaging screen. The immunoprecipitates were run on an identical gel and western blotted to identify the precise position of immuno-precipitated MOEP19. Although MOEP19 was recovered in the immunoprecipitates from both oocytes and 2 cell embryos as evidenced by its identification on the Western blot, there was no evidence on the autoradiograph that immunoprecipitated MOEP19 incorporated radioactive methionine, despite incorporation of radiolabel into many proteins at both stages.

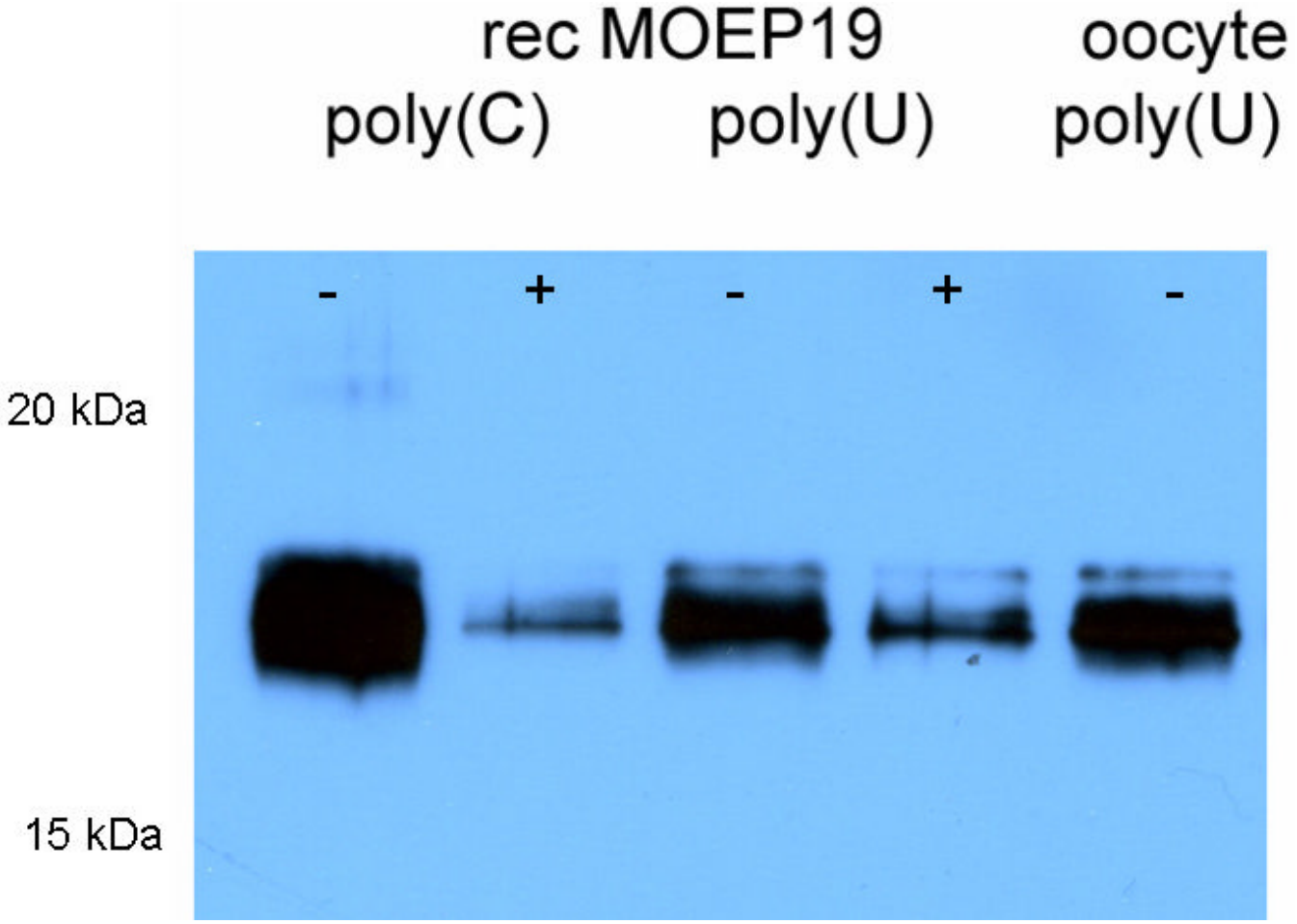

Fig. 14.

Autoradiograph of Western blot developed by chemiluminsecence after probing with anti-MOEP19 serum. Recombinant and endogenous oocyte MOEP19 were eluted from polynucleotide beads with (+) or without (-) pre-incubation with poly (U). Purified recombinant and endogenous MOEP19 bound to both poly (U) and poly (C) ribonucleotide homopolymers. The binding to poly (U) was competed by pre-incubation with poly (U).